Exploring the optimal conditions for the infiltration and immobilization of colloidal activated carbon in sandy aquifers for subsurface groundwater treatment

By Max Lamberts BSc (5630940)

1st supervisor: dr. Niels Hartog, Utrecht University and KWR Water Research Institute
2nd supervisor: Enno de Vries MSc, Utrecht University

Master Thesis
Program Earth Surface and Water
Utrecht University, Faculty of Geosciences
And KWR Watercycle Research Institute

June 26-6-2020

Abstract

Due to the growing world population and the resulting increase in the amount and diversity of micro pollutants in surface and groundwaters, conventional water treatment methods are more and more unable to provide sufficient pollutant removal. Against this background, it is important that water treatment technologies are improved or new advanced technological developments are developed to keep water treatment effective and sustainable. Near well subsurface groundwater treatment is a recent idea to enhance water treatment in an effective and economical way. With this technique, the reactivity of the sediment around a pumping well is enhanced with a reactive material to create a reactive zone around the pumping well. A suitable reactive material for this purpose is activated carbon colloids (ACC) since these colloids are small enough (<10 µm) to be transported through a porous system, it's effective against a wide range of micro pollutants and it is chemically stable. In their natural state, these colloids tend to coagulate. To inject ACC's into the aquifer, stabilization of the suspension is essential. However, the mobile suspension has to immobilize in the subsurface so that it is not returned during subsequent abstraction. In this study, we aimed to further explore the possibility of ACC as an agent for near well subsurface treatment. Batch suspension tests were conducted to determine the ACC stability on different variables like ACC types, pH, ionic strength, carboxymethyl cellulose (CMC) concentration and mixing intensity. This was followed by column experiments where the different suspensions and their performance in a saturated porous was analyzed. A high suspension stability was obtained in high pH (10.6-11) deionized water and with addition of CMC. A high mixing intensity also increases suspension stability significantly. The creation of a reactive zone over the full length of the column was obtained using high pH deionized water and CMC as stabilizers. However, when CMC was used as a stabilizer, a larger decrease in hydraulic conductivity (K) of the sand was observed. The decrease in K was also larger when the flow velocity was reduced. In the remaining experiments where high pH deionized water as a stabilizer was used, the decrease in K was minimal. These results suggest that pH deionized water is a promising method for the stabilization of ACC's in suspension, intended for infiltration in the subsurface with the goal of creating a reactive zone.

Acknowledgements

I would like to thank my supervisors Niels Hartog and Enno de Vries for their guidance and advice during my thesis and their understanding during Corona times and giving me the time to finish my thesis properly. Niels, the weekly talks were very constructive and useful and helped me stay on track during the process. Also thanks to Martin van der Schans for accompanying us at the weakly talks and giving his input and thanks to all other coworkers at KWR for creating a nice and friendly work environment.

Furthermore I would like thank my friends who were also writing their master thesis for the fun coffee breaks and good conversations in the Vening Meineszbuilding. Last I want thank Tessa for the support during stressful times and my parents for their ever going support.

Contents

1 Introduction

Clean and safe drinking water is a vital necessity for life. With increasing global population, climate change and increasing water pollution, the pressure on the availability of fresh water for drinking water production increases. Recently, media have been writing about the challenges The Netherlands and the Dutch drinking water companies have to face, to keep the drinking water quality as high as it is nowadays (Volkskrant, 11-9-2019 & NOS, 12-9-2019). These problems do not only occur in The Netherlands, but areas around the whole world are facing drinking water quality problems (Hanak et al., 2015; Li & Guo, 2019). Due to increasing rural activity and the use of pharmaceuticals, both developed and developing countries are facing an increasing amount and diversity of micropollutants in their ground and surface water (Houtman et al., 2014; Gehrke et al., 2015; Sjerps et al., 2017; Sjerps et al., 2019). Although conventional water treatment methods have proven to be effective since their implementation, it has also become clearer that in the current state of affairs these methods are becoming insufficient (Gehrke et al., 2015; Kümmerer et al., 2019). Advanced water treatment techniques like sonolysis, UV photolysis and reversed osmosis are better at treating some pollutants but they also have their limitations. The costs and the energy use of these techniques are high and they can cause for the creation of new unwanted products from the original pollutants (Gupta et al., 2012 ; Kümmerer et al., 2019). Innovations in water treatment technology are therefore still necessary to achieve sustainable and cost-effective ways for drinking water production.

The use of nano technology in water treatment techniques offers new opportunities to enhance the treatment process. The past few decades, a large number of nano particle based in-situ groundwater remediation techniques have been developed (Obiri-Nyarko et al., 2014; Faisal et al., 2018). The most common particulate reactive materials for in-situ groundwater remediation include nano zero valent iron (nZVI), zeolites and activated carbon. The reactivity of these material has been well investigated as well as their suitability for in-situ remediation (Newcombe et al., 1993; Park et al., 2002; Fu et al., 2014; Fan et al., 2017). A popular technique is to create permeable reactive barriers of the reactive material, that intercepts the contamination plume (figure 1). One of the difficulties in in-situ remediation is that the particles of the reactive material have to be brought into the aquifer. This has proven to be a difficult task as the ratio of pore space to particle size or grainsize to particle size determines whether particles are small enough to be transported through the pores. Depending on other aquifer characteristic like heterogeneity and surface roughness of the grains, particle size to grain size ratio should vary around 0.0017-0.003 for particle transport through the porous medium (Bradford et al., 2002; Bradford et al., 2003; Bradford et al., 2007).

nZVI for subsurface groundwater remediation has been widely researched and is able to immobilize and destroy or reduce contaminants like chlorinated organic compounds, nitroaromatic compounds, arsenic, heavy metals, nitrates, dyes and phenols by way of redox reactions (Thiruvenkatachari et al., 2008; Fu et al., 2014; Faisal et al., 2018). nZVI particles are small enough to enter a porous media, needed for in situ remediation. However, nZVI tends to agglomerate very easily so pretreatment of a nZVI is necessary. The stabilization of nZVI suspensions has been done using a polymer called carbocy methyl cellulose (CMC). CMC is the most used and researched polymer for this goal (He et al., 2009; Zhan et al., 2009). CMC causes for steric repulsion between particles making it harder for the particles to coagulate. These CMC stabilized nZVI particles, tested in sand filled columns and in the field, were able to be transported through the porous medium with minimal to no clogging of the pores (He et al., 2009; Busch et al., 2014; Kocur et al., 2014; Busch et al., 2015). Activated carbon (AC) used for in-situ groundwater remediation is in the form of activated carbon colloids (ACC). These ACC's can be as small as 0.1 µm (Sorengaard et al., 2019). AC is a chemically stable material making it very suitable for subsurface remediation as it doesn't alter the chemistry of the aquifer (Thiruvenkatachari et al., 2008). AC is able to adsorb dissolved organic matter (DOM) and other organic substances, aromatic compounds, pathogens, medicines and certain metals to its surface. Due to its porous structure, it has

a very large surface area available for adsorption (Perrich, 1981; Smeets et al., 2009; Sharme & Bhattacharya, 2017). As these ACC's tend to coagulate when untreated, it is difficult to inject them into a porous medium with small pores. CMC is considered as a stabilizer for ACC as well. Georgi et al. (2015) evaluated the suspension stability of ACC suspensions treated with carboxy methyl cellulose (CMC) and humic acid. They concluded that CMC is a very good stabilizer for several AC based products. There are also several commercial AC based products available on the market for in situ remediation. Products like Plumestop and Carbon Iron CMC have been applied in the field multiple times (Regenesis, 2016) but a detailed independent documentation of their effectiveness in the field is lacking (Fan et al., 2017)

A more recent idea in water treatment technology is near well subsurface groundwater treatment. This technique aims to create a reactive zone around a pumping well by using a reactive material (Hartog, 2016) (Figure 1). AC is a good reactive material for this purpose because it is chemically stable and it is effective against a wide range of MP's (Thiruvenkatachari et al., 2008; KWR, 2018). Instead of a remediation technique focusing on the source of a contamination, this technique is applied as a water treatment technique for the production of clean water. One advantage of this technique is that it would be possible to target wells with contamination problems, and to pretreat this contamination before the water of this pumping well is mixed with raw water from other wells at the water treatment facility. Another advantage is that when a new pumping well is constructed and there is no treatment plant in the vicinity, treatment in the subsurface may be sufficient for some purposes of the water like agricultural use. The bottleneck in creating a reactive zone, is to get the AC in a radius around the well in the subsurface and to ensure that it stays there. For the AC to enter the porous sand body, the

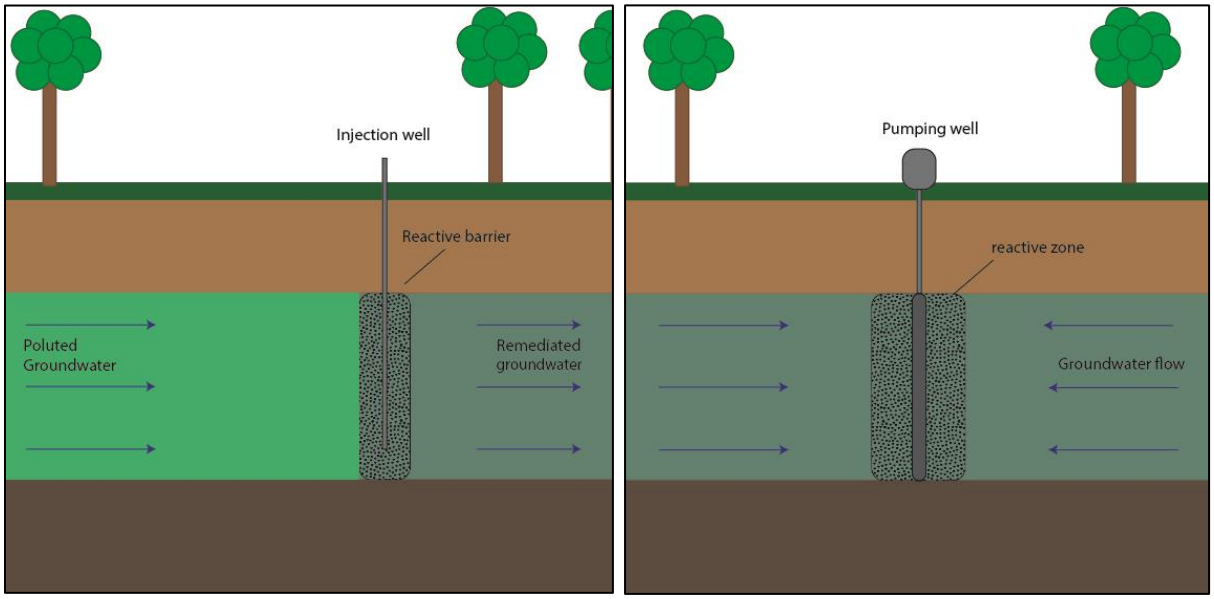

Figure 1: Schematic representations of subsurface groundwater remediation using a reactive barrier (left) and near well subsurface groundwater treatment (right).

particles must be mobile and small enough to travel through the pores. However, at some distance from the well, the particles should immobilize to avoid pumping them back up with the water. A study conducted by KWR (2018), explored the applicability of ACC for the creation of a reactive zone around a pumping well. They found that CMC works as a good stabilizer for ACC suspensions but ACC's were too mobile to immobilize in a sand filled column. The creation of a reactive zone in the column was achieved, when passing an ACC suspension through an ultrasonic bath.

In this study, we aimed to further explore the possibility of ACC as an agent for near-well subsurface treatment by assessing ACC suspension stability and mobility and immobilization processes in sand filled columns. The main goals and research questions are:

- What is the stability dependence of an ACC suspension for different variables:ACC types, pH, ionic strength, CMC concentration and mixing intensity and?
- Can it be expected that for a stable suspension, dispersion/ dilution at the injection front eventually leads in the immobilization of the activated coal particles?
- Conduct macroscale column experiments to test the injection of the identified most promising suspension conditions.
- What is the effect of different ACC suspensions and injection rate on the immobilization of the ACC's and the permeability of the sand body?
- How can the findings of the research help in towards the implementation in practice?

In order to answer these research questions, lab experiments were conducted. The first part of the experiments consisted of several batch jar tests in which the suspension stability of an ACC suspension is assessed. The second part of the lab experiments consisted of column experiments to see how the best performing ACC suspensions from the first part will infiltrate into a sandy body. In these experiments the ACC suspension is injected into a saturated sand column where different scenarios are tested. Lastly, the results are put into broader perspective to analyze how our findings can help to find the optimal circumstances to create an AC based reactive zone around pumping wells.

2. Theory of suspension stability

2.1 DLVO theory

In order to create a stable suspension, coagulation between the particles in the suspension should be minimal. The colloidal interaction is best explained by the DLVO theory that addresses the inter surface forces and factors that play a role in these colloidal interactions (Stumm, 1992; Hunter, 1993, Trefalt & Borkovec, 2014). It also helps us understand the interaction between particles and another surface like the grains of a sandy porous medium. Whether colloids coagulate is the result of the sum of the attracting forces and the repulsive forces between the particles (Stumm, 1992; Hunter 1993).

The attractive forces between two of the same particles are often mainly determined by the relatively weak Van der Waals forces. The Van der Waals forces depend on particle properties and distance between the surfaces of the concerning particles and are independent on the solution chemistry (Trefalt & Borkovec, 2014).

The repulsive forces (figure 2) are the result of the surface charge and the electrostatic double layer that is formed around the particles as a result of the charge of the particle (Trefalt & Borkovec, 2014; Olson, 2012). The electric state of a charged surface depends on the free electronic or ionic charges available. A charged surface attracts counter ions, ions that are of the opposite charge. These counter ions order themselves around the charged particle in such a way that there is a layer of counter ions attached to the surface called the Stern layer. Around this Stern layer is the so called diffuse layer, which is a layer enriched in counter ions, but these ions are not all adhered to the surface. They are attracted by the opposite charge of the particles, but they also experience the repulsion of the like-

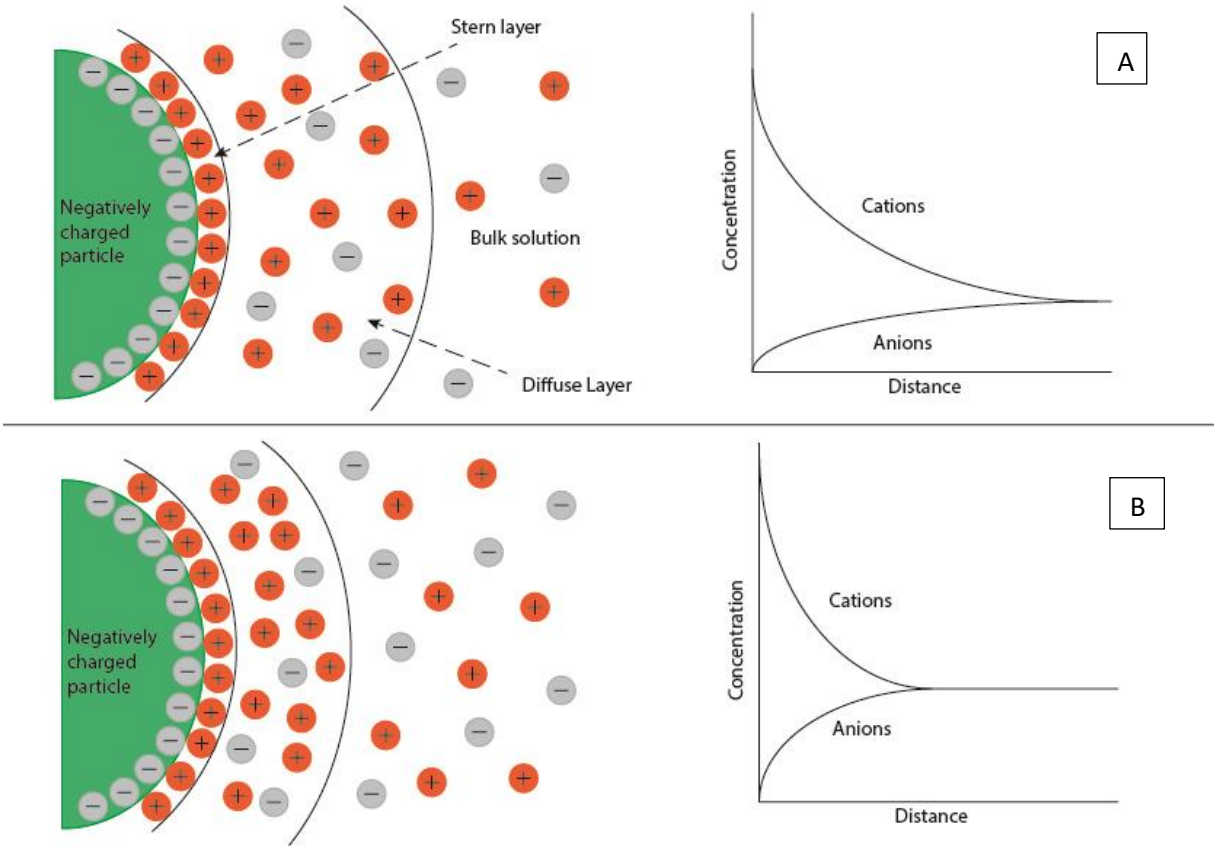

Figure 2: Schematic representation of the distribution of ions around a (negatively) charged particle. B shows the same situation with a higher ionic strength of the solution. Notice that the diffuse layer is repressed by the ions in the bulk solution.

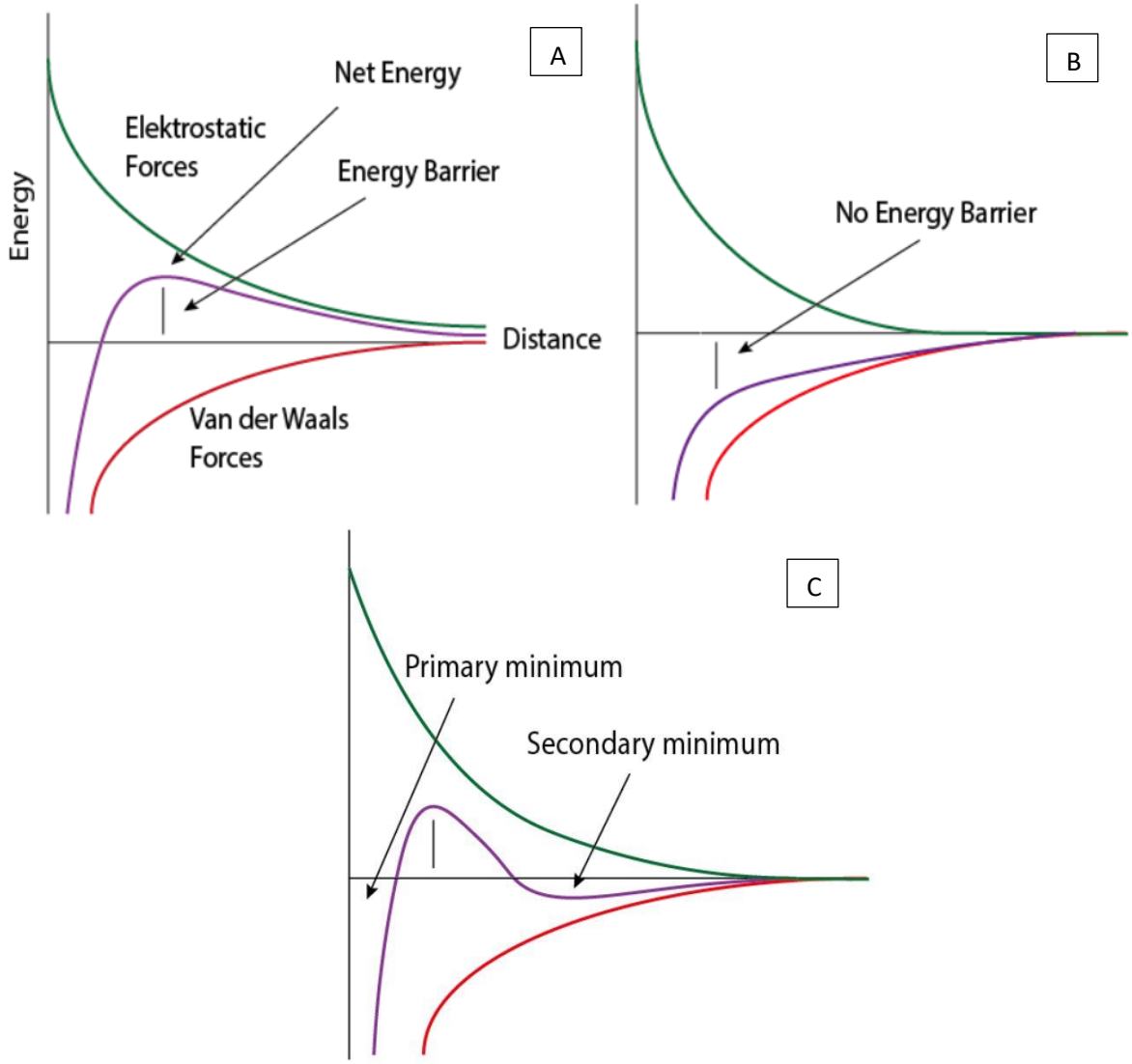

Figure 3: Net energy with distance from the charge particle. [A] electrostatic forces stay high enough to counter the Van der Waals forces at a certain distance, creating an energy barrier, preventing the particles from coagulation. [B] electrostatic forces decline to fast to create an energy barrier. [C] A secondary minimum occurs after the energy barrier, attraction in the secondary minimum is less strong than in the primary minimum.

charged ions in the Stern layer. Beyond the diffuse layer there is the bulk solution in which the distribution of positive and negative ions is equal (Figure 2). The thickness of the double layer can be approximated by the Debye length (1/κ) (Trefalt & Borkovec, 2014):

$$\kappa^{-1} = \sqrt{\frac{k_B T \varepsilon_0 \varepsilon}{2000 e^2 N_A I}} \qquad [1]$$

Where k_B is the Boltzman constant, T is the temperature, ε_0 is the dielectric constant, ε is the permittivity, e is the elementary charge, N_A is the Avogadro's number and I is the ionic strength of the solution. The ionic strength of a solution is given by (Trefalt & Borkovec, 2014):

$$I = \frac{1}{2}\sum_i z_i^2 \, [i] \qquad [2]$$

i are all the types of ions in the solution, z_i is the valence of the ion type and *[i]* is the concentration in moles per liter. As can be seen from the equations, the ionic strength plays a major role in the value of the Debye length. All the other components are constants except for the temperature. However differences in temperature changes are often negligible as they often vary a few degrees around 293 K. differences in ionic strength are far larger and therefore far more influential on the Debye length.

The thickness of the double layer and the surface charge of the particle are very important in determining whether particles coagulate or stay free. Figure 3 shows a schematic of the force balance with distance from the colloid. Close to the surface, van der Waals forces are very strong as they are dependent on the distance from the surface. Further away from the surface, the van der Waals forces decrease. This the same for the repulsive electrostatic forces. Close to the surface they are strong, but not as strong as the Van der Waals forces, and they decrease with distance from the charged surface. The steepness of decrease in these repulsive forces is dependent on the thickness of the double layer (Hahn & Omelia, 2004). This results in a net attractive or repulsive force for a certain distance from the surface of the particle. If at some distance from the surface, the repulsive forces become larger than the attractive forces, an energy barrier is formed, preventing the particles from coagulation (Figure 3A). Only if there is enough kinetic energy to overcome this energy barrier, the particles can coagulate. If there is a net attractive force and the van der Waals forces are for every distance from the surface larger than the repulsive forces, coagulation will occur (Figure 3B). Another option is that after the occurrence of an energy barrier, the net forces become attractive again, resulting in a so called secondary minimum. Particles that are bound in the secondary minimum are referred to as flocculated instead of coagulated. Attraction in the secondary minimum is less strong than in the primary minimum and less energy is needed to bring particles back into suspension again (Stumm, 1992; Olson, 2012; Trefalt & Borkovec, 2014).

2.2 The effect of pH and ionic strength on suspension stability and zeta-potential

The electrostatic repulsion between particles is often expressed as the zeta-potential. The zeta potential is a key parameter for suspension stability and is the electric potential at the interface of stern layer and the double layer (figure 2). A high zeta-potential means a high suspension stability. The zeta-potential is mainly dependent on the pH and the Ionic strength of the suspension.

The magnitude of the surface charge of a particle is mainly controlled by the dissociation of surface groups and is dependent on the pH of a suspension. A surface can obtain a positive or negative charge depending on the pH (figure 4). The pH where the net charge of the particle is zero is known as the iso-electric point or the point of zero charge (pzc) (figure 4). Repulsive forces and zeta potential increase with decreasing and increasing pH from the pzc. The pzc is dependent on the particle characteristics (Salgin et al., 2012; Trefalt & Borkovec, 2014;).

The surface charge of a particle is also dependent on the ionic strength of the solution as more ions in the solution means more potential for surface group dissociation (figure 4). However, as mentioned before, the ionic strength plays a larger role in the thickness of the diffuse double layer around the particle. The idea is that with a larger ionic strength, the amount of free ions in the bulk solution is higher. This results in the compression of the double layer by the free ions in the double layer (figure 2). Due to the compression of the double layer, the layer becomes thinner meaning the extent of the repulsive forces is lower. Thus relatively strengthening the van der Waals forces and weakening the electrostatic forces at every distance from the particle (figure 5) (Stumm, 1992; Trefalt & Borkovec, 2014). The specific relationship between zeta-potential and ionic strength is for every particle different but zeta potential always decreases with increasing ionic strength.

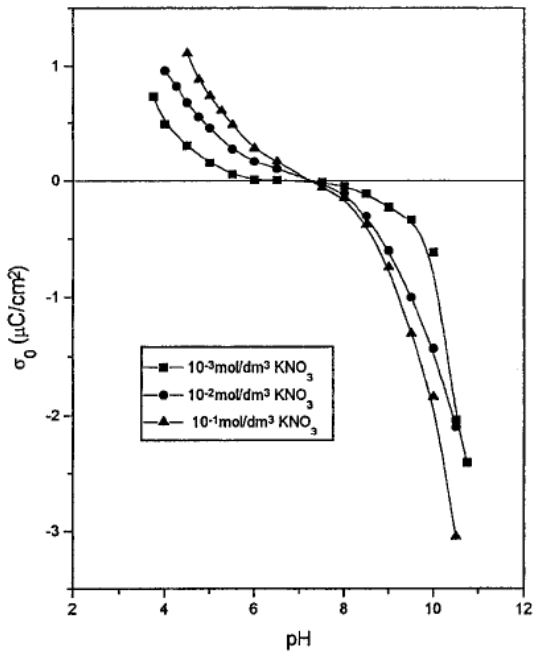

Figure 4: The surface density of activated carbon colloids (ACC) as a function of pH in KNO3 solutions with different concentrations (Babic et al., 1999). The pzc is the point where the graphs intersect the x-axis. With an increase or decrease in pH from the pzc, the surface charge density also increases. The higher the KNO_3 concentration, the higher the surface charge density.

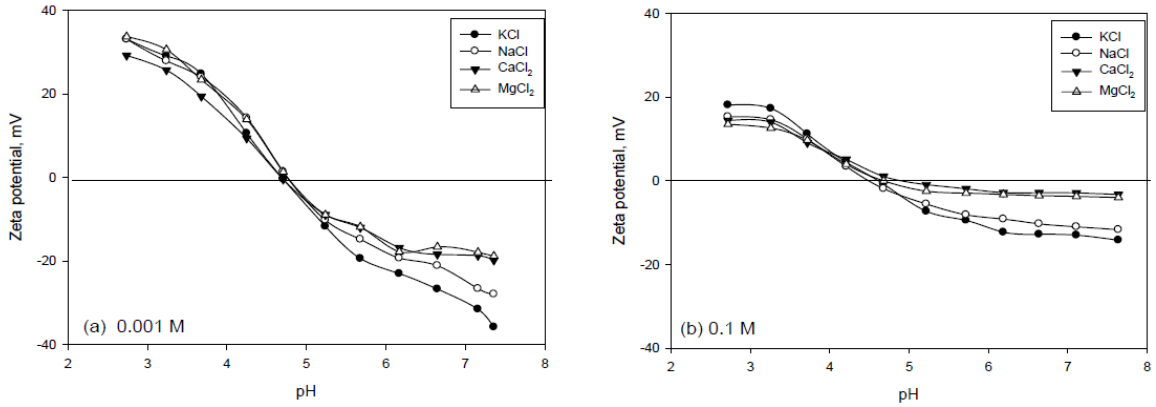

Figure 5: Zeta potential of bovine serum albumin (BSA) biomolecules as a function of pH (Salgin et al., 2012) in 0.001M (left) and 0.1M (right) salt solutions. The figure shows a higher zeta potential with a lower salt concentration (left) and also shows that ions with a higher valence have a more negative effect on the zeta potential.

2.3 Electrosteric stabilization

Electrosteric stabilization is the stabilization of particles by adsorption of polymers like CMC, on to the particle's surface. This polymer has an ionizable group that dissociates in the solvent to create a charged polymer. The adsorption of polymers onto the surface of the particle results in an adsorbed layer giving rise to repulsive forces between particles with adsorbed layers (Napper, 1977). Suspension that are sterically stabilized remain stable even in high ionic strength and conditions where the zeta potential would normally be very low.

3. Methods & materials

3.1 Batch suspension stability tests

The first part of the lab experiments existed of testing the stability of ACC suspensions under various conditions. The different suspensions varied in pH, ionic strength, and CMC+ACC concentration. To study the suspension stability, jar tests were performed. A jar test is a method often used in water treatment technology to evaluate the ideal flocculation circumstances for flocculation as a method for water remediation (Hogg 1999; Krasner & Amy, 1995; Microdyn Nadir, 2017).

3.1.1 pH dependence

The first condition tested, was the stability dependence of the ACC in suspension on pH. A 500 ml solution was made in a 1 liter beaker with deionized MilliQ-water and the desired amount of NaOH or HCl was added to get to the right pH range. After the solution was made, 0.5 g (1g/L) ACC of manufacturer CABOT Corporation, product NORIT SA UF, was added to the solution and stirred by a magnetic stirrer for 15 minutes. The suspension was sampled 90 minutes after stirring with a pipette from the upper layer of every suspension to analyze the turbidity. The turbidity was measured with a HACK 2100Q (chapter 3.1.1). After sampling, the pH of the suspension was measured with a pH meter. In the beginning the pH of the solution was measured before the addition of ACC. However, it was noticed that the ACC also altered the pH of the water. Therefore, pH was subsequently measured at the time of taking the sample.

The same tests were also conducted for the ACC types NORIT SAE SUPER and NORIT ASPEC E 153 also from manufacturer CABOT Corporation (table 1). These types did not show promising results (see results) so the subsequent experiments were only conducted with the NORIT SA UF product.

Table 1: Specifications and description of the tested types of powdered activated carbon (cabotcorp.com, 2020)

Product	D_{10}(µm)	D_{50}(µm)	D_{90}(µm)	Total Surface Area (M^2/g)	Description
NORIT SA UF	-	5	-	1200	"Powdered activated carbon with superior kinetics and ultrafine particle structure. It is ideally suited for use with hollow fiber ultrafiltration membranes in potable water treatment."
NORIT SAE SUPER	-	20	-	1050	"Powdered activated carbon developed for wastewater treatment. It is a highly activity grade with strong adsorptive capacity for low and high molecular weight organics (color bodies, chemical oxygen demand and organic micropollutants).
NORIT ASPEC E 153	1	4	10	-	"Medium coloring power E 153 activated carbon black colorant for food and cosmetics."

3.1.2 Ionic strength dependence

To examine the effect of the ionic strength on the suspension stability, sodium chloride (NaCl) was added to the solution to alter the ionic strength of the solution. An amount of NaCl equal to 0.01 moles/L and 0.1 moles/L was added to the solution. These concentrations of NaCl were chosen as they are both representative ionic strength values for fresh groundwater (Wallace et al., 2012; Rietra et al., 2004). The suspension was again sampled 90 minutes after stirring with a pipette from the upper layer. The tests were also conducted in tap water, which also has a higher ionic strength than MilliQ water, but the ionic strength was unknown. However, ionic strength can be estimated from the electrical conductivity (EC) using the following simple relation (Ponnamperuma et al., 1966):

$$I \approx 0.016 * (EC) \quad [3]$$

Where *I* is in *mol/L* and *EC* is in *mS/cm*. The EC was not measured, but from a water quality overview from the drinking water company (VITENS) a minimum EC of 0.257 mS/cm and a maximum EC of 0.309 mS/cm was measured for the effluent water from the treatment plant, intended for tap water at the lab location for the period the experiments were conducted (Waterkwaliteitsoverzicht Tull en het Waal, 2020). This means that the ionic strength of the tap water was probably between 4.11 mmol/L and 4.94 mmol/L.

3.1.3 CMC Stabilization

The effect of CMC as a stabilizer was measured for different concentrations of CMC based on literature (Georgi et al., 2017; KWR BTO, 2018). Concentrations of 20 mg/L, 50 mg/L, 100 mg/L, 200 mg/L and 250 mg/L were assessed. It was observed that CMC is relatively hard to dissolve in water, so a diluted CMC solution was prepared using a blender. First the amount of ACC was added to tapwater after which the desired amount of diluted CMC solution of 1 g/L was dropped into the suspension while it was stirred on a magnetic stirrer. This was also compared with mixing the ACC suspension with CMC in a blender.

3.1.4 Turbidity used as an indicator of suspension stability (NTU)

Turbidity is a property that is linked to the cloudiness of a solution/suspension and is measured in NTU (nephelometric turbidity unit). It is caused by the scattering of the light by particles in the solution. More particles means thus more light scattering and thus a higher turbidity (Austin, 1973). If more particles are stable in suspension and less particles are settled, the measured turbidity will be higher. The settling of particles is influenced by the size of the particles and aggregation/coagulation of particles. Coagulated/flocculated particles are larger and settle faster than small, single particles (Eisma, 1986).

The turbidity can be measured using a nephelometer, which measures the side scattering of a light beam colliding with a particle. This is not the true value of light scattered by the particle but it has been showed that the side scattering is in fairly constant ratio with the total scattering (Kirk, 1994). Here we used a HACH 2100Q for turbidity measurements.

To quantify the turbidity for ACC in suspension, with the unit NTU, the relation between ACC concentrations in the water and measured turbidity was determined by bringing a known amount of ACC into suspension in MilliQ water by a magnetic stirrer. Immediately after the magnetic stirrer was turned off, a sample was taken from the water column to measure the turbidity with the HACH 2100Q. This way, the concentration ACC in suspension was known and could be linked to the turbidity. This

procedure was repeated for different water qualities, taking pH, with/without CMC, tap water and stirring intensity into account.

3.2 ACC suspension column infiltration experiments

The second part of the lab work consisted of column experiments with the goal of assessing the mobility and retention of the ACC's and the creation of a reactive zone for different ACC suspensions.

3.2.1 The Corle sand

The sand originated from the subsurface at a groundwater pumping location near Corle the Netherlands. The sand is a coarse heterogeneous sand with an estimated median grain size of 420-600 µm based on a sand ruler. The sand contains also larger grains up to small gravel. A more precise grain size analysis could not be carried out anymore due to the restrictions regarding the Corona-crisis. This specific sand was chosen for several beneficial reasons. First, The light color of the sand is in good contrast with the black ACC. This way the location and quantity of the ACC immobilization is well visualized. Secondly this sediment is rather clean and doesn't contain a lot of organic matter, silt or clay. This is important in the possibility of creating a mass balance to investigate the amount of ACC passing through the sand column and the immobilized portion of ACC inside the column. Lastly, the hydraulic conductivity of the sand is also a representative value for drinking water aquifers.

3.2.2 The column set up and preparation of the column

After some testing and getting familiar with the material, the following test set-up was conducted (figure 6). A column with a length of 85 cm and a diameter of 3.5 cm was packed with Corle sand for every scenario. One pore volume was equal to the volume of the column times the porosity of the sand (0.35) plus the volume of the tubes as the water had to pass through the tubes as well before it is measured. The amount of pore volume was found to be around 395 ml. The inlet of water was attached at the top of the column and the outlet at the bottom to induce downward flow in the column. The influent water and suspension was infiltrated from a plastic container with a nozzle underneath it where the tube was connected to. The nozzle was on the inside extending beyond the bottom of the container so that the ACC that settled on the bottom was not utilized for infiltration into the column. On the outlet of the column, a tube directed the effluent water to a beaker standing on a scale, so the discharge during a time interval was monitored constantly. We assume the density of water to be 1000 gr/L.

Flow through the column was induced by a head difference. Flow by a head difference was preferred over flow by a peristaltic pump, as a peristaltic pump results in pulsating flow and thus not a constant injection rate. Pulsating flow would not be representative compared to a constant flow. Also, using flow induced by a head difference makes it possible to monitor the hydraulic conductivity during the experiment. If the hydraulic conductivity decreases due to the infiltration of ACC, the discharge through the column will decrease as well. A constant head test was conducted to constantly measure the hydraulic conductivity between time intervals. The head difference was between the 145 and 155 cm but only varied around 1 cm in the time interval discharge was monitored. This drop in hydraulic head during a time interval was neglected as is this was far smaller than the total head difference. The hydraulic conductivity was determined with a constant head test, using the following equation:

$$K = \frac{Q}{A} * \frac{L}{H} \qquad [4]$$

Where *K* is the hydraulic head, *Q* is the discharge, *A* is the cross-sectional area normal to the flow, *L* is the length of the column and *H* is the hydraulic head.

The preparation of the column started with the filling of the column with sand. There was a constant layer of water for the sand to fall on, preventing the trapment of air in the pores. The sand was topped of with a small layer (2 cm) of filtersand. During an initial test it was noticed that some sand got pushed into the tube during reversed flow because of the smaller particle size. The filled column was flushed with alkaline water and tapwater to get the residual mobile OM, clay and silt out of the column to prevent these particles from influencing the turbidity measurements and the measurements for completing the mass balance (see 3.2.4). After this, the column was flushed with normal tapwater

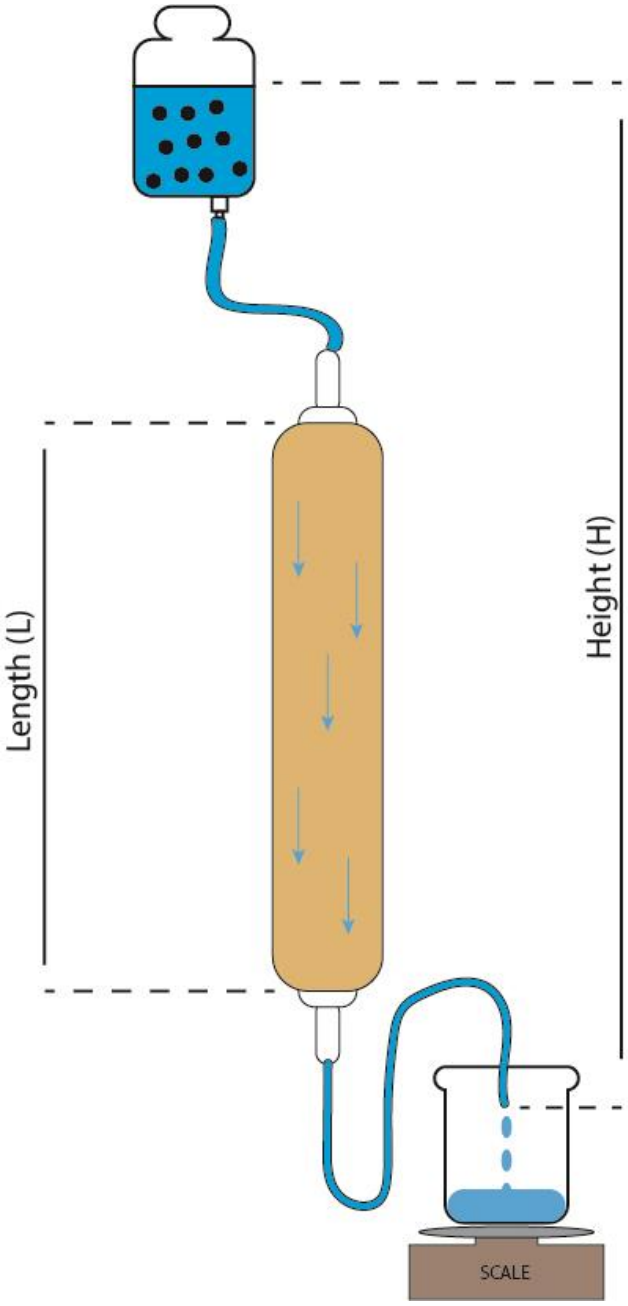

Figure 6: experimental setup for the column experiments.

untill the turbidity of the water was around 1 NTU, equal to the turbidity of normal tapwater. During the flushing with tap water, the hydraulic conductivity of the sand and discharge through the column was also monitored.

3.2.3 The suspensions

It has become clear from the suspension tests that there are several factors playing a role in the stability of a suspension. These factors should be taken into account when running the column tests and the effect in change of these factors should be addressed. The injected suspensions differ per scenario but are prepared the same way. The intended amount of CMC solution or NaOH solution was added and mixed with the water by a magnetic stirrer. Afterwards, the intended amount of ACC Norit SA UF was added while mixed with the magnetic stirrer. The suspension tests showed that the mixing intensity had a clear effect on suspension stability as well. So the suspensions were also mixed in a blender to mix them thoroughly. This should increase the initial amount of uncoagulated ACC's per ACC suspension. Table 2 shows the tested suspensions.

Table 2 Tested suspensions in the column. Every suspension was 1.5 liters of ACC suspension. Front and back injection meant an injection of 0.5 pore volume of alkaline deionized water (pH 10.6) before and after the ACC suspension was injected.

Scenario	ACC concentration (gr/L)	Water	Stabilizer	Initial Darcy flow velocity (m/hour)	Mixing	Front and back injection
1	2	Tap water	-	4.2 ± 0.2	Blender	-
2.1	2	MilliQ	20 mg/L CMC	4.2 ± 0.2	Blender	-
2.2	2	MilliQ	200 mg/L CMC	4.2 ± 0.2	Blender	-
3	2	MilliQ	20 ml NaOH → pH 10.6	4.2 ± 0.2	Blender	-
4	2	MilliQ	20 ml NaOH → pH 10.6	4.2 ± 0.2	Blender	yes
5	1	MilliQ	20 ml NaOH → pH 10.6	4.2 ± 0.2	Blender	-
6	2	MilliQ	20 ml NaOH → pH 10.6	2.5	Blender	-
7	2	Tap water	-	4.2 ± 0.2	Ultrasonic bath	-

The above mentioned scenarios were based on the results from the suspension tests and literature. Scenario 2.1 was chosen from the results of the batch suspension stability experiments, 20 mg/L already had a significant effect on the suspension stability. Scenario 2.2 was based on results of Georgi et al. (2015). They concluded that 2.5 g/L CMC for an amount of 11 g/L ACC resulted in a stable suspension. This is equal to 500mg/L CMC for 2 gr/L. However, their suspension had a higher ionic strength (5 mM Ca^{2+}) and such a high concentration of CMC increases the viscosity of the water as well. That's why a lower concentration of 200 mg/L was chosen, still 10 times higher than scenario 2.1.

As the results of the suspension tests showed a higher suspension stability for water with a high pH, several scenarios (3-6) with a suspension with a high pH were conducted. It was also investigated what

the effect of a front and back injection of alkaline water (scenario 4), ACC concentration (scenario 5) and infiltration velocity (scenario 6) is.

At last, the effectiveness of an ultrasonic bath as pretreatment was investigated. This option was considered based on the BTO rapport of KWR (2018).

For every scenario, 1.5 liters of ACC suspension was prepared but only around 1.3 liters of this was utilized in the experiment. Due to the design of the plastic container from which the ACC suspension was infiltrated into the column, a part of the suspension was always left behind. The outlet of this container was higher situated than the bottom of the container, so everything beneath this height could not leave the container. This was partly done on purpose, as this way, more coagulated ACC was excluded from entering the column.

3.2.4 The experimental process

During every test, several things were monitored. The effluent discharge was regularly monitored to monitor the hydraulic conductivity.

The turbidity of the effluent was regularly monitored to construct a relative break through curve (BTC) of the ACC. This was compared with actual flow velocity to see if there was retardation of the ACC suspension.

Pictures of the column were made regularly as well, to visualize the evolution and formation of the zone where the activated carbon immobilizes.

After the infiltration of the suspension, the column was flushed about 2 times the pore volume until the turbidity was around 1 NTU again to make sure the fraction of ACC in suspension that was not immobilized was fully flushed out. After the flushing, the column was also flushed the other way to simulate pumping and investigate if this doesn't disturb the created reactive zone and mobilizes the immobilized fraction again.

The effluent water, the water that passed through the column during the backflushing and the part of the ACC suspension that was not infiltrated into the column were collected to make a mass balance of the passed ACC fraction, immobilized ACC fraction and remobilized ACC fraction. A part of the ACC also stayed behind in the tubes so the tubes were also flushed into the collected fractions. The collected amount of water was filtered and the filtered amount of ACC was weighed to determine the concentration in the collected water and thus complete the mass balance.

3.3 Comparing velocities in the column with radial flow around a well

To translate the infiltration velocities in the column experiments to field scale pumping well some simple calculations were conducted. With typical measurements of a pumping well and the corresponding flow velocities as described in KWR rapport (van der Schans & Meerkerk, 2019) it is possible to make an indication for flow velocities in the zone around a well. Flow velocities around the borehole can not be to high to prevent the transport of sand, silting up of the filter and (bio-)chemical clogging of the filter. The maximum allowed Darcy flow velocity at the borehole wall that drinking water companies in the Netherlands often use in practice, is dependent on the hydraulic conductivity and is determined by the equation of Huisman:

$$q_{borehole} = \frac{\sqrt{K}}{30} \qquad [5]$$

Where $q_{borehole}$ is the maximum allowed flow velocity (m/s), *K* is the hydraulic conductivity in m/s. This also means that there is a maximum allowed discharge for a pumping well that can be calculated by:

$$Q = 2 * \pi * r * L * q_{borehole} \quad [6]$$

Where Q = the discharge, r = the radius of the borehole, L the length of the filter.

There are two other methods for calculating the maximum allowed velocity at the borehole wall. The formula of Sichardt was widely used in the past and is given by:

$$q_{borehole} = \frac{\sqrt{K}}{15} \quad [7]$$

For heat cold storage systems in the Netherlands, they often work with a subtraction norm of the NVOE (van der Schans & Meerkerk, 2019) and is given by:

$$q_{borehole} = \frac{K}{12} \quad [8]$$

Where *K* is in m/day and $q_{borehole}$ in m/hour.

4. Results and Discussion

4.1 Batch suspension stability tests

4.1.1 Relation between turbidity and concentration

Figure 7 shows that various linear relations between the turbidity and concentration exist depending on the mixing intensity and potential stabilizers added to the suspension. Whereas a suspension with a higher pH, gives a higher turbidity for the same concentration and same mixing intensity. When the mixing intensity is increased, the gradient also increases and becomes similar for the different suspensions mixed in the blender. When mixing intensity is this high, the stabilizing effects in the suspension seem to become negligible indicating that the suspension is fully dispersed.

This means that turbidity cannot be directly linked to concentration, except if the suspension is directly measured after mixing. When particles get the time to coagulate, the relation between concentration and turbidity will shift. The turbidity and concentration have a linear relation only under similar circumstances and if the moment of measuring the sample is the same. A lower turbidity will be measured when the ACC particles are more coagulated than when the particles are separated for the same concentration. More free particles are able to reflect more light from the nephelometer.

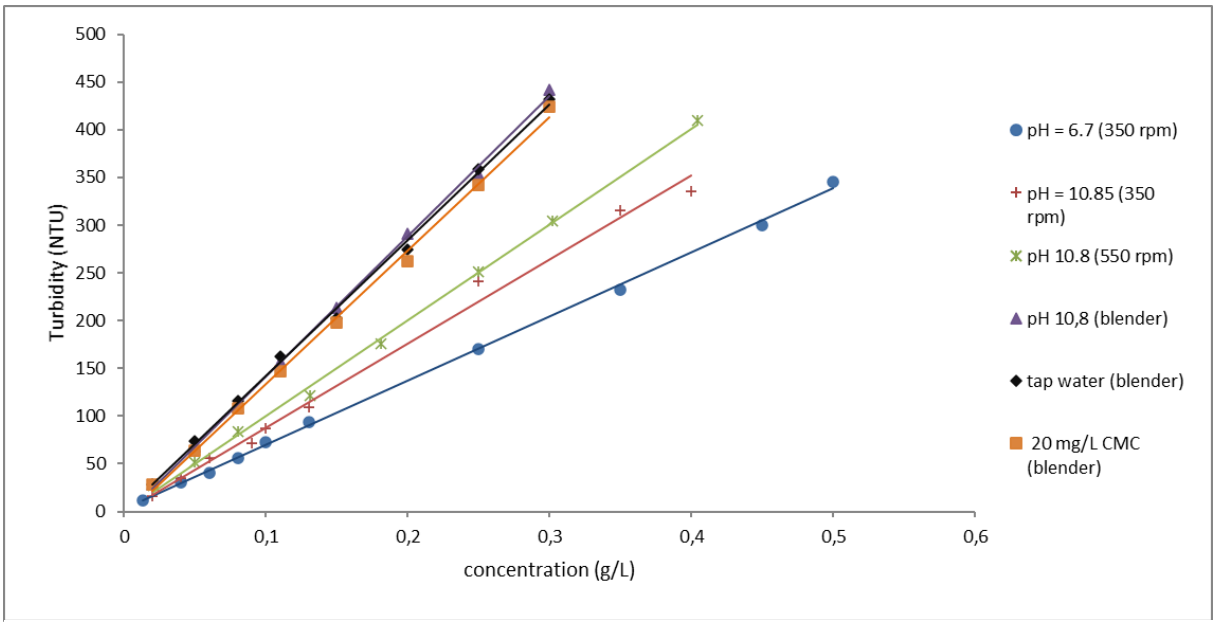

Figure 7 Linear relation between turbidity and ACC concentration. The linear relations all had a high determination coefficient, with the lowest R2 = 0.9929.

4.1.2 Effect of pH on turbidity

The batch suspension stability tests showed a higher turbidity for the different ACC suspensions at a higher pH (figures 8A, 8B & 8C). Figure 9 shows also visually that for an ACC type NORIT SA UF suspension at pH 10.07 the suspension is much darker after 90 minutes.

The results showed differences in suspension stability for the different ACC types in ultra-pure deionized Milli-Q water. The largest variation and highest stability at high pH was seen for the type NORIT SA UF (figure 8A). For this type, the turbidity for suspensions with a pH higher than 10.7 was mostly too high for the nephelometer to measure. The used nephelometer should be able to measure up till 800 NTU. However, for these ACC suspensions, every measurement above 413 NTU was unmeasurable for the nephelometer. This seemed to be dependent on the characteristics of the ACC

suspension since the nephelometer was able to measure higher turbidity values for the included suspensions used for calibration and for the breakthrough curves (section 4.2.2). For the unmeasurable high data points on figures 8A and 10 the turbidity is set at the 500 NTU line for graphical readability of the figures. Regarding the two other ACC types NORIT SAE SUPER and NORIT ASPEC E153 The same pattern of a higher turbidity after 90 minutes is observed (figure 8B & 8C). However the absolute values of turbidity are far lower. Both SAE SUPER and ASPEC E153 have a turbidity between the 90 and 100 NTU around pH 11,5. At neutral and low pH ASPEC E 153 suspension shows particularly low turbidity of 25 and lower.

These differences in suspension stability between different ACC types is consistent with previous research. Bjelopavlic et al. (1998) studied the surface charge of 7 different types of AC at different pH's and found different points of zero charge for the different AC types an Chingombe (2005) also measured different zeta potentials and points of zero charge for different ACC types. This indicates that ACC properties play an important role in choosing the right ACC type. From the three ACC types tested here, the NORIT SA UF showed the most promising results. NORIT SAE SUPER has a larger d_{50} than NORIT SA UF and NORIT ASPEC E153 (table 1) with faster settling of the particles as result. The application of NORIT ASPEC E153 as a food coloring product might be the reason why suspension stability is less for this ACC type since this type is not designed as a reactive material. Furthermore, the shape of the ACC particles can play a role in suspension stability (Kim et al., 2015).

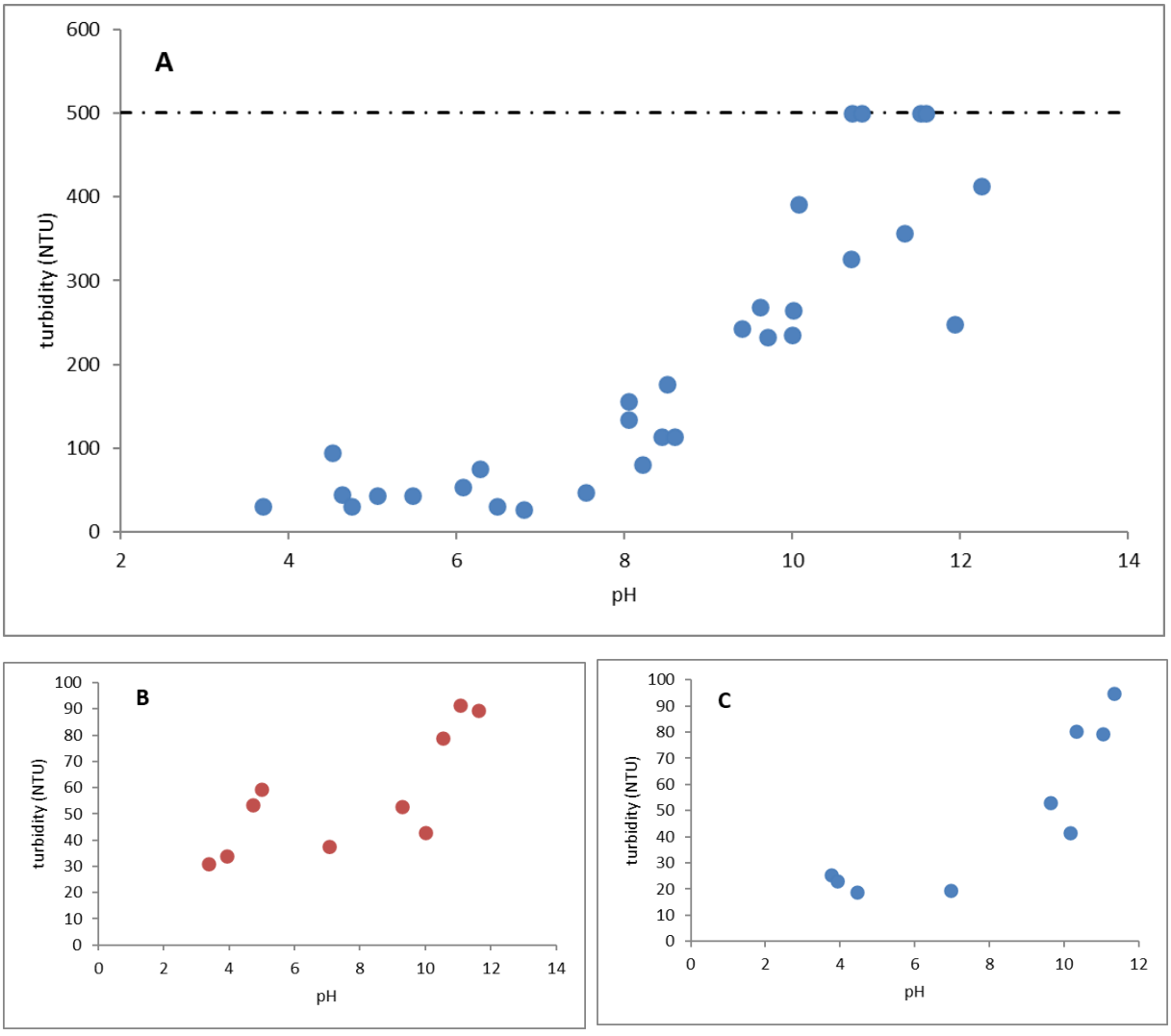

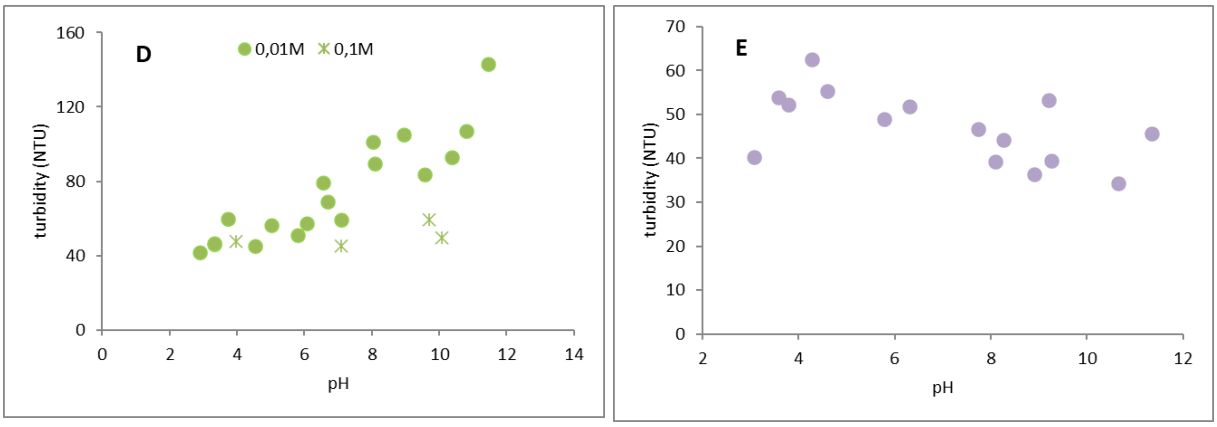

Figure 8 Turbidity measured at different pH's after 90 minutes of settling for different ACC types and different solutions. [A} NORIT SA UF in MilliQ water, [B] NORIT SAE SUPER in MilliQ water, [C] NORIT ASPEC E153 in MilliQ water, [D] NORIT SA UF in MilliQ water with addition of NaCl, [E] NORIT SA UF in tap water (I ≈ 4.11-4.94 mmol/L) . The maximum value of 500 NTU for some of the cases in figure 1A is to point out that the turbidity was too high for the nephelometer to give a real value.

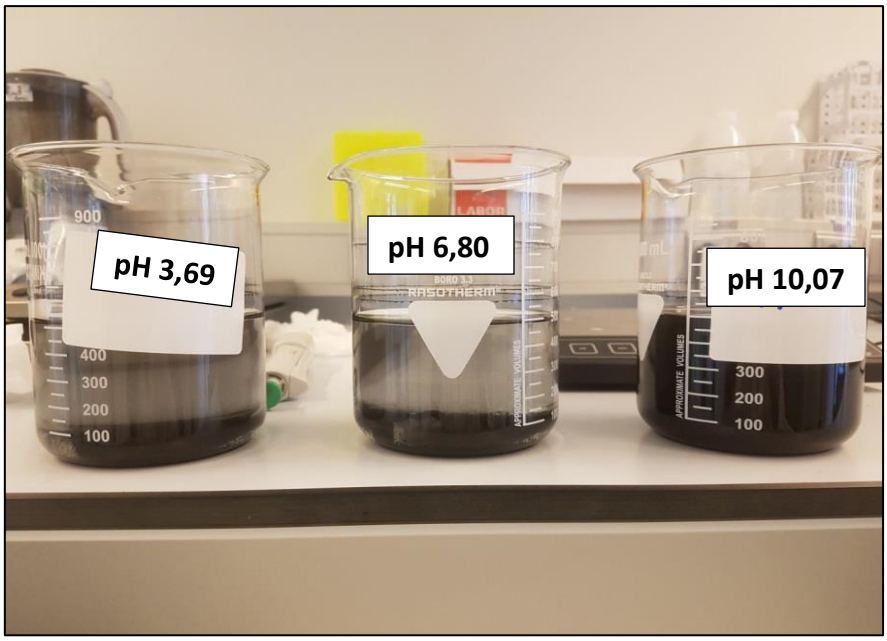

Figure 9 Examples of the turbidity for ACC suspensions at different pH after 90 minutes. The suspension is clearer for the suspensions at pH 3,69 and pH 6,80 compared to the dark black suspension at pH 10,07.

4.1.3 effect of ionic strength on turbidity

The ionic strength of the suspension plays a major role in the suspension stability. In the NORIT SA UF suspension with an ionic strength of 0.01M, the turbidity at high pH clearly decreased (figure 8D) relative to the suspension with deionized water (figure 8A). However, turbidity at high pH is still higher compared to neutral and low pH. An increase in ionic strength to 0.1M results in an even lower turbidity (figure 8D). This matches with the DLVO theory and other studies where the stability of ACC suspensions was assessed (Newcome et al., 1993; Basar et al., 2003). Suspensions made in tap water also show a low turbidity for the full range of pH assessed (figure 8E). There is no clear distinction in turbidity between neutral, low and high pH while initial ionic strength for the tap water is probably lower than the suspension with I = 0.01M. However, ionic strength at lower and higher pH than the starting pH of the tap water, differs from the initial estimated ionic strength. Bicarbonate (HCO_3^-) is one of the major ions in the tap water but reacts with OH^- to H_2O and CO_3^{2-} at increasing pH. This way, the ionic strength is increased because CO_3^{2-} is a multivalent ion (equation 2). The other way around, with decreasing pH HCO_3^- reacts with H^+ to H_2CO_3 which does not have a charge, decreasing the ionic

strength. Beside that, there are more multivalent ions like Ca^{2+} in the tap water that have a larger effect on the diffuse double layer (Trefalt et al., 2017).

4.1.4 The effect of stirring on the suspension stability

A higher initial mixing intensity results in a longer settling time and a higher turbidity for a longer time (figure 10). For this, settling over time was compared for different suspensions mixed with a blender or by a magnetic stirrer (350 rpm). The turbidity after the same time interval was for the suspension mixed with the blender higher than the suspensions mixed with the magnetic stirrer.

For the suspensions mixed with a magnetic stirrer, it can be seen that the decrease in turbidity over time can be described by some sort over power function. Settling is fast at first and slows down over time.

In the case of CMC stabilized suspension mixed with the magnetic stirrer, the turbidity starts of at a lower turbidity but the decrease in turbidity over time is less. The diluted CMC solution was probably still not mixed well by the magnetic stirrer. Because, when this same solution was mixed with the blender, the suspension stability was far higher for a longer time period. The same was the case for a high pH suspension mixed in the blender. Apparently the mixing intensity not only causes for a better dispersion of the particles initially (figure 7, see 4.1.1) but also over a longer time period. The initial separation of the particles means they have to pass the repulsive barrier for them to coagulate again. Once separated, it is harder for the particles to coagulate and once coagulated also more energy is needed to separate them again.

It was also noticed that when a suspension was longer exposed to the atmosphere, this had an effect on the turbidity and settling time. Therefore, a high pH suspension with 15ml/L NaOH was created and the turbidity was monitored over time for a situation open to the atmosphere and one situation in a

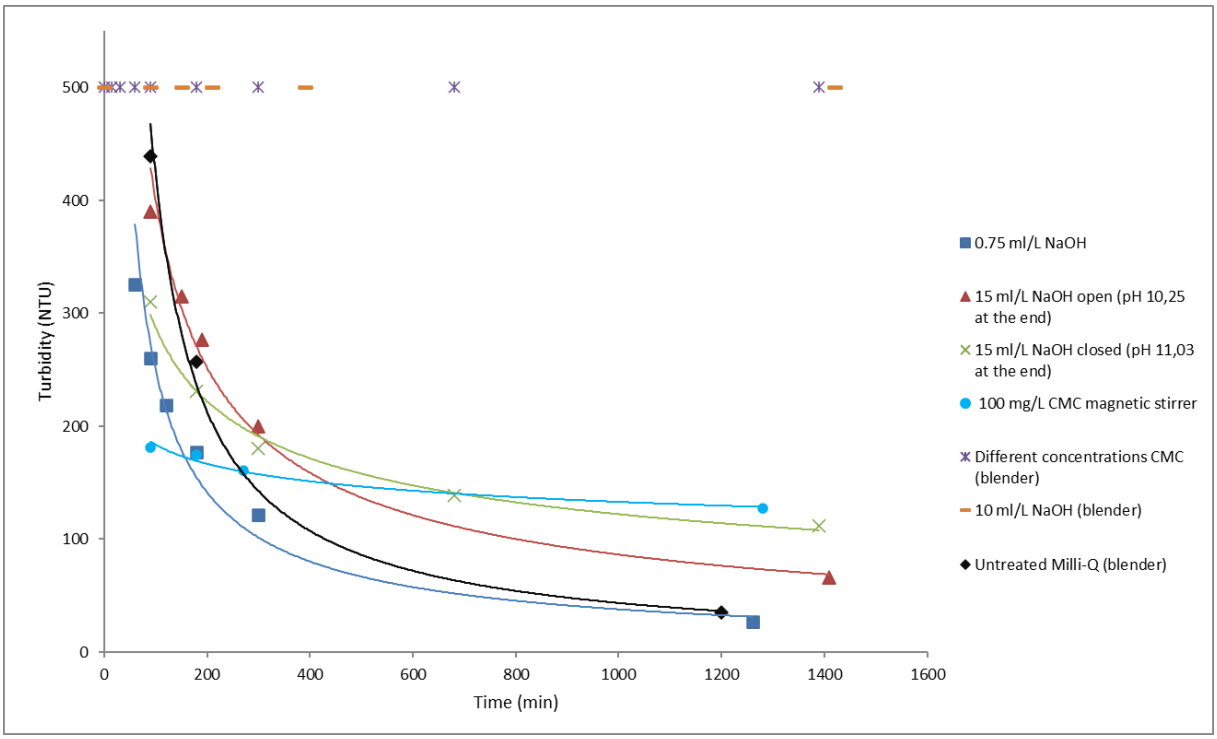

*Figure 10 Suspension turbidity over time for different cases. The following power functions were fitted by excel: 0.75 ml/L NaOH gave turbidity (T) = 10826*minutes (m)-0,819 with R2 = 0.9755, 15 ml/L NaOH open gave (T) = 8538,7*(m)$^{-0,665}$ with R^2 = 0.9915, 15 ml/L NaOH closed gave (T) = 1591,9*(m)$^{-0,665}$ with R^2 = 0.9915, CMC magnetic stirrer gave (T) = 350,06*(m)$^{-0,14}$ with R^2 = 0.9711, mixer untreated Milli-Q water (T) = 39547*(m)$^{-0,986}$ with R^2 = 0.9966.*

closed jar (figure 10). Although the high pH suspension closed to atmosphere started at a lower turbidity after 90 minutes than the suspension open to atmosphere, the decrease in turbidity over time was slower for the situation closed to the atmosphere. This is probably the result of the deionized water equilibrating with the air and CO_2 to dissolve in the water with the result of more free ions in the bulk solution. Besides, the pH of the suspension open to atmosphere had dropped from 11.41 to 10.25 at the end while the pH of the suspension closed to atmosphere dropped from 11.39 to 11.03. This is because CO_2 is a weak acid as well, lowering the pH in the suspension open to atmosphere and therefore lowering the suspension stability.

4.2 Column experiments

4.2.1 Mass Balance

A mass balance was constructed from the collected and weighted ACC's during every step in the experiments.

Using a stabilizer (scenario 2.1 – 6) resulted in a larger portion of the ACC to pass the full length of the column (figure 11). Although the effluent in these scenarios was turbid (figure 12) and thus contained an amount of ACC, the total weight of these particles was very small. Only the smallest particles, stable in suspension, managed to pass the whole sand column. The weight of these particles was so small that a scale accuracy down milligrams, was unable to measure the weight accurately. Only around one weight percent or less of the ACC particles passed the entirety of the sand column. It could also be seen during the experiment that the particles passing through were very small. Instead of being able to recognize lose particles in suspension, the effluent had a black cloudiness to it. The relation between turbidity and ACC showed in figure 7 is therefore also not in accordance with the passed through ACC in suspension. As mentioned before, small particles in the same concentration as larger particles, are able to reflect more light in the nephelometer. However they probably have a quantitative relation to each other.

Figure 11 also shows that the use of a stabilizer for the ACC suspension (scenario 2.1-6) plays a large role in how much ACC is infiltrated and retained in the column. Pretreatment of the ACC suspension results in less settling in the bulk solution before it is infiltrated in the column thus more ACC is utilized. Especially the scenario's treated with a high pH (scenario 3 and 4, figure 11) show a large portion of the ACC to be used for infiltration and is retained in the column. This ratio of infiltrated ACC and not utilized ACC is the same for the suspension with half the concentration (scenario 5, figure 11). The ratio immobilized/not utilized for scenario 3 is 1.42 and for scenario 4 1.40. This indicates that the portion settling in the bulk solution is not dependent on concentration for these concentrations. The factors playing a role in this are the stability of the suspension and the injection time. In the case of scenario 6, the injection time was longer because of the lower flow velocity, so the ACC suspension also had more time to settle in the bulk solution resulting in a lower fraction of ACC that was infiltrated in the column.

A small but significant portion of the ACC is remobilized again during reversed flow. It was observed that during the experiment part of the ACC did not really infiltrate into the sand but stayed on top of the layer of filter sand. This portion of ACC got largely flushed back. Also a large portion of the ACC immobilized in the small layer of filter sand during infiltration, got flushed out during reversed flow. The portion of remobilized ACC was significantly smaller in the case of CMC. This layer of ACC on top of the filter sand also formed in these scenarios but did not remobilize as easily. It was noticed during the experiments with CMC stabilized suspensions (scenario 2.1 & 2.2) that, although the suspension seemed stable beforehand, some sort of flocculation in the column occurred. This observation has not been mentioned by earlier research using CMC as a stabilizer for ACC's (Georgi et al., 2015; Regenisis,

2016; KWR, 2018). However, CMC generally has a stabilizing effect but bridging flocculation by CMC is also a possibility. In this case, a single polymer molecule absorbs onto two or more ACC's, thereby connecting the colloids (Du et al., 2007). Whether bridging flocculation occurs is dependent on CMC and particle concentrations and doesn't have to occur for the whole suspension.

In all the tested scenario's a significant part of the ACC in the suspension was not infiltrated in the column (figure 11). Due to the design of the plastic container containing the bulk suspension, ACC that settled at the bottom, was not utilized for infiltration.

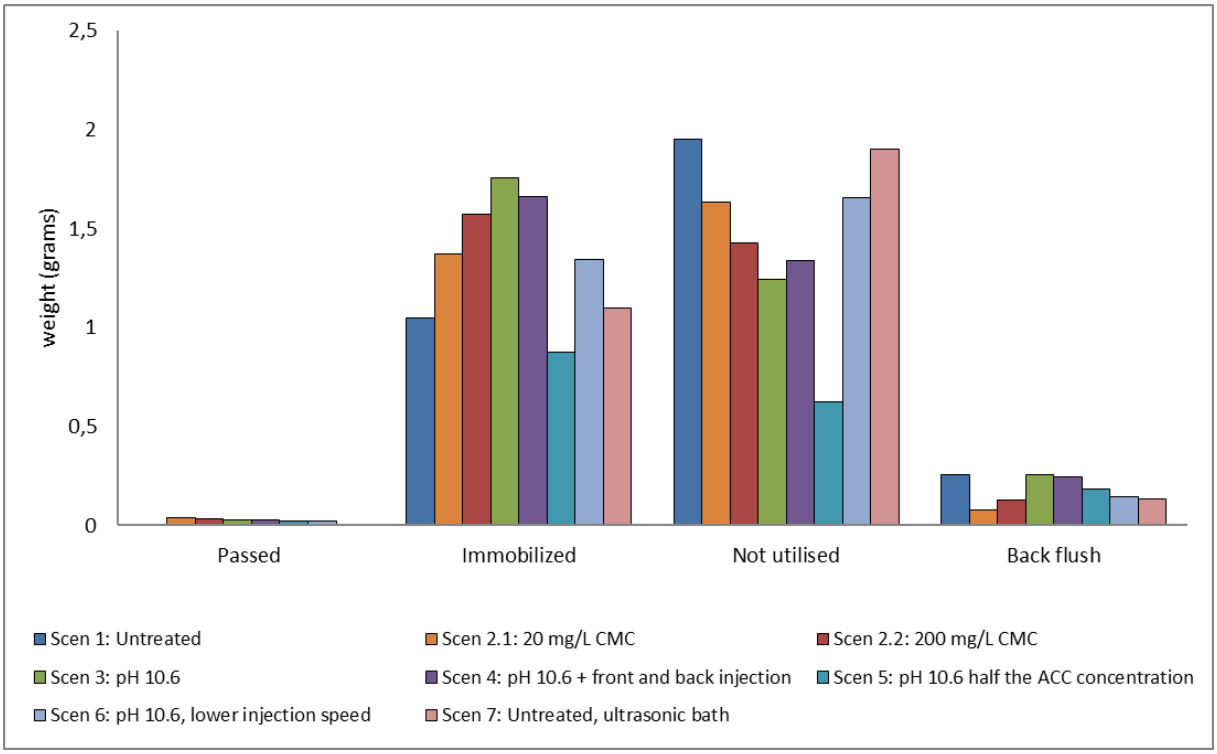

Figure 11 A mass balance of the used ACC per scenario. The figure shows the weight of the fraction that passed the column, the fraction that was immobilized in the column, the fraction that was not used and stayed behind in the bottle and inlet tube and the fraction that got mobilized again during reversed flow. The bars of infiltrated and not used count up to 3 gram, the total amount of ACC used per scenario. Except for scenario 5 where the total amount of ACC used was 1,5 gram

4.2.2 Breakthrough curves and passed ACC

In the case of all the chemically stabilized ACC suspensions, a fraction of the ACC's passed the column. This resulted in a breakthrough curve for these scenarios (figure 12). The breakthrough takes around 3 – 3.5 pore volumes, which is also equal to the infiltrated volume of ACC suspension. This implies that flow in the column occurred through the sand and that there was no flow along the sides of the column. All the breakthrough curves start around 1 pore volume or before 1 pore volume. In the case of scenario 2.1, the breakthrough seems to start earlier. This is probably not the case and is the result of the large time interval between 2 measuring points. The BTC's also didn't show any tailing and stopped around 1 pore volume after ACC injection was stopped. This implies that there is no significant remobilization of particles. There was no breakthrough of ACC for the unstabilized suspension which corresponds with the mass balance (figure 11). This indicates that CMC and high pH as stabilizers make ACC's more able to travel through the pores without immobilization.

The break through curves of scenario's 2.1, 2.2 and 6 show a different course than the curves of scenario 3, 4, and 5. In the case of scenario 3, 4 and 5 the curves show a rather fast and steep increase until a certain turbidity at which it stays stable at this turbidity until it decreases again. For both the

scenario's where CMC was used (scenario 2.1 and 2.2) and the scenario where the flow velocity was reduced (scenario 6), there is a gradual increase up until the point the curve decreases again. Bradford et al. (2002) noticed this same phenomenon researching the transport of carboxyl particles through sand bodies. They also observed the normal BTC's and the gradual increasing BTC's. They accounted the gradual increase to a superposition of straining and attachment to the sand. Straining is the immobilization of colloids by the trapping in the pore throats. It is important here to make a distinction in complete straining or mechanical filtration and incomplete straining. Complete straining is the complete retention of the colloids at the soil surface and occurs when the particles are large enough to block major pore throats with a significant reduction in permeability as a results. incomplete straining occurs when there is only straining in pores smaller than some critical size. In this case, major pore throats stay active and the reduction in permeability is smaller (Bradford et al., 2002 ;Bradford et al., 2006). Incomplete straining results in the skewed BTC's observed in figure 12. The course of the skewed BTC's is explained by that there is more straining in the beginning of the experiment and the first cm's of the column. The blocking of the smaller pore throats results in dead ends in the first cm's of the column, trapping colloids travelling this path. This results in a higher retainment of particles at the beginning of the experiment. When the dead ends are filled up, only the larger continuous pores are utilized for the transport of the colloids. The increased straining when CMC is used (scenario 2.1 and 2.2) can probably also be assigned to the bridging flocculation mentioned earlier (section 4.2.1). According to Bradford et al. (2007) the increased straining also occurs when injection velocity is reduced, like in scenario 6, as a result of the decreased fluid drag forces due to a reduction in flow velocity.

Although figure 7 cannot be used to obtain a concentration from the breakthrough curve, There probably is this same relative linear relation between the different BTC's and the concentration. This means, a double as high turbidity is also a double as high concentration. This is also backed up by the mass balance in figure 11 where the amount of AC that passed through the column was higher in the scenario's using CMC.

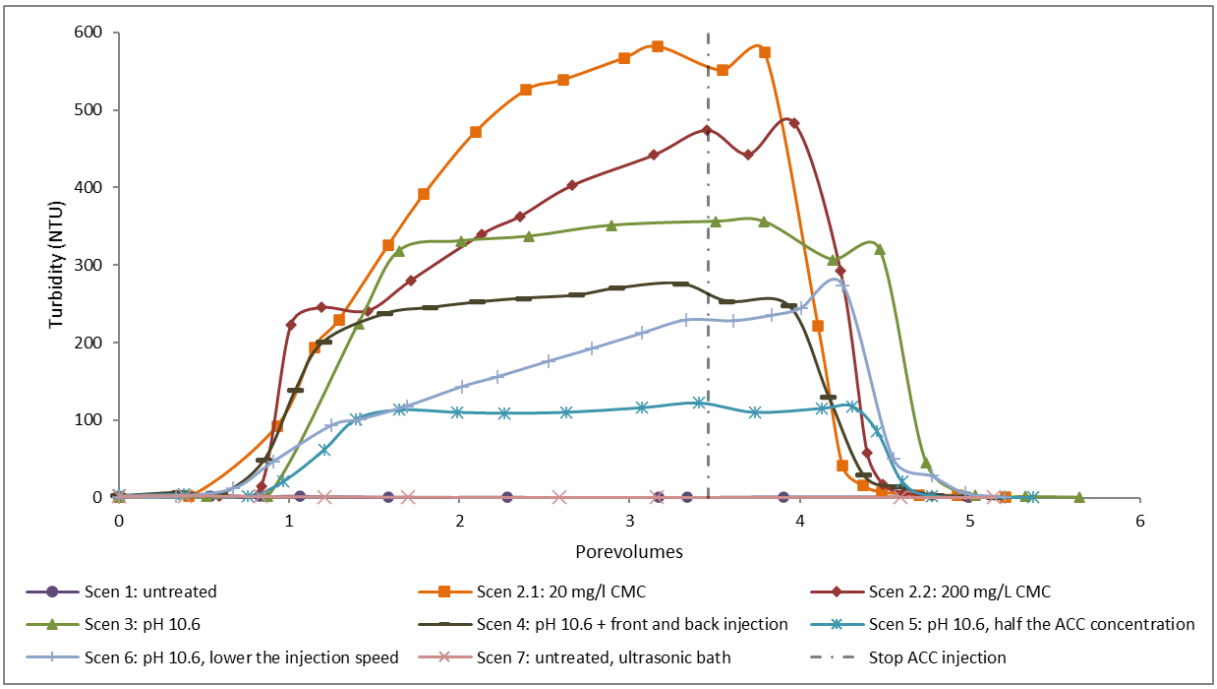

Figure 12 Break through curves of ACC passing the column expressed in turbidity against pore volumes. The turbidity gives a relative indication of the amount of ACC suspension passing through the whole column. The dotted vertical line gives the average moment the injection of ACC suspension stopped.

There is a slight dip visible, at the end of each curve. This is around the moment the injection of the ACC suspension is changed with water again. During this switch, the experiment is stopped for a moment (30 seconds) and apparently this has some effect on the turbidity of the passed water. This dip seems to be more pronounced when the turbidity is higher and is likely the result of the immobilization of some particles as a result of the pause in flow.

4.2.3 Hydraulic conductivity change

The average hydraulic conductivity of the sand in the column was 59.8 m day^{-1}. However, there was some variation in starting hydraulic conductivity between the different scenario's. This was probably due to differences in packing, the effectiveness of the flushing or differencing in the sand of the used sand core. The lowest K value was 55 m day^{-1} in the case of scenario 4 and the highest K value was 63.3 m day^{-1} for scenario 5.

Changes in K were monitored during the experiment to see if clogging occurred and to what extent (figure 13 A). In every scenario K was lower at the end of the experiment. During the ACC infiltration, a gradual decrease in K is observed. However, the magnitude of the decrease differs per scenario. The scenario's where the suspension was pretreated with CMC show a larger decrease in K than the other scenarios (figures 13 A & B and 14). Scenario 2.1 shows a very large decrease in K and scenario 2.2 shows a larger than average decrease in K). Also a lower flow velocity/infiltration speed seems to result in a larger decrease in K as is the case in scenario 6. This also substantiates that in these scenario's immobilization of the ACC by straining is higher. Straining reduces the permeability of the sand body due to the closing of pore throats.

The decrease in K is especially limited in scenario's where no stabilizer was used (scenario 1 and 7) and also the decrease in K per gram ACC is here the smallest (figure 13 B). This seems in contrast with what is expected as the particles are more prone to coagulation with more straining as a result. A possible explanation might be that because the suspension is not stabilized, a pre selection of only small particles takes place in the container containing the batch suspension. The larger particles and coagulated particles settle out faster and only the smaller particles are used for infiltration into the column.

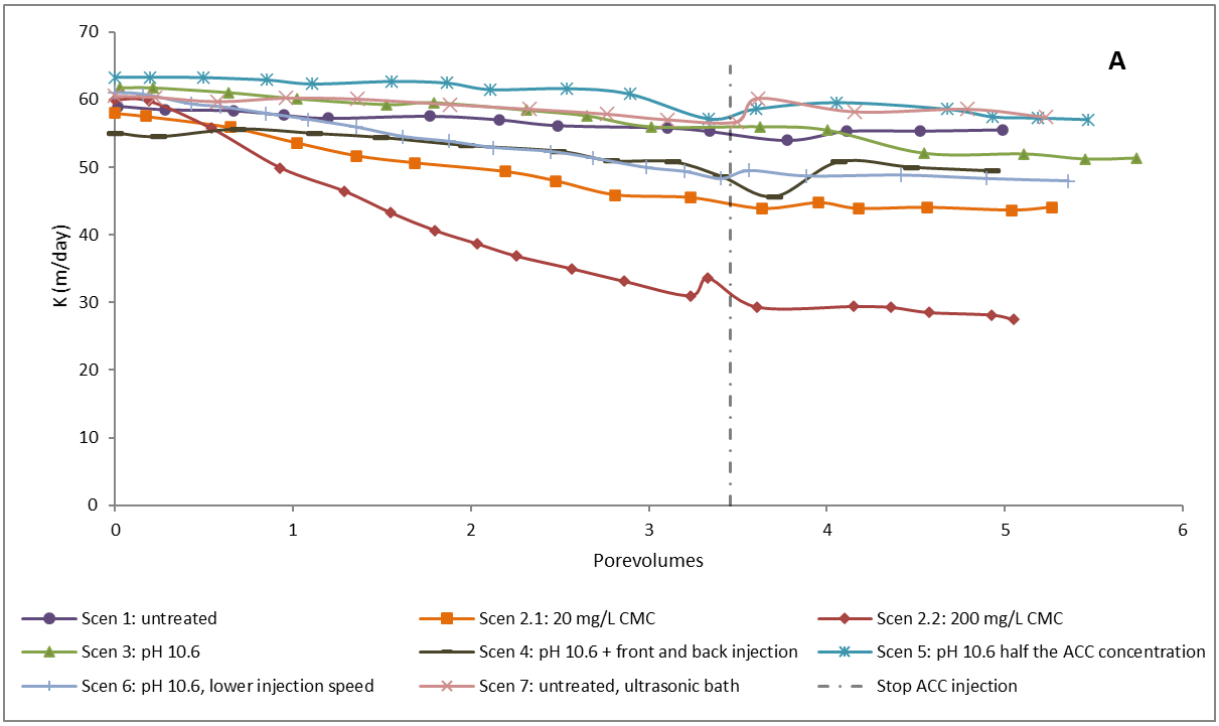

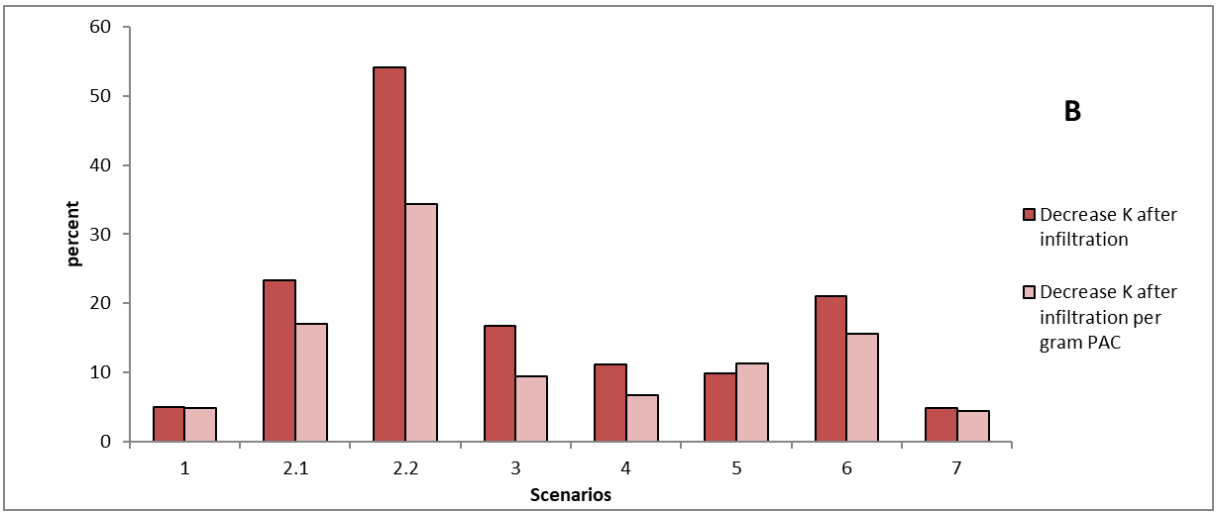

Figure 13 A: The evolution of K during the length of the experiment for the different scenario's tested. B: The total decrease of K as a percentage of the starting K and the decrease per infiltrated gram of ACC.

A front injection of high pH water to delay the contact of between the ACC suspension front and the water in the column seems to have minimal effect. The total relative decrease in K and the decrease per gram ACC are both lower in scenario 4 than in scenario 3. However, the difference is rather small and therefore the significance should be questioned.

Although the K decreases in every scenario during infiltration of ACC, K is often partially restored when flow direction is reversed (figure 8). Apart from scenario 1, K during reversed flow is higher than at the end of the infiltration. In scenario 4 and 7, K in reversed flow is even higher than the original K value during the infiltration flow direction. It is likely that during reversed flow some of the strained pores are opened up again, increasing the permeability. The K value did not change during the reversed flow and stayed constant from the moment flow started.

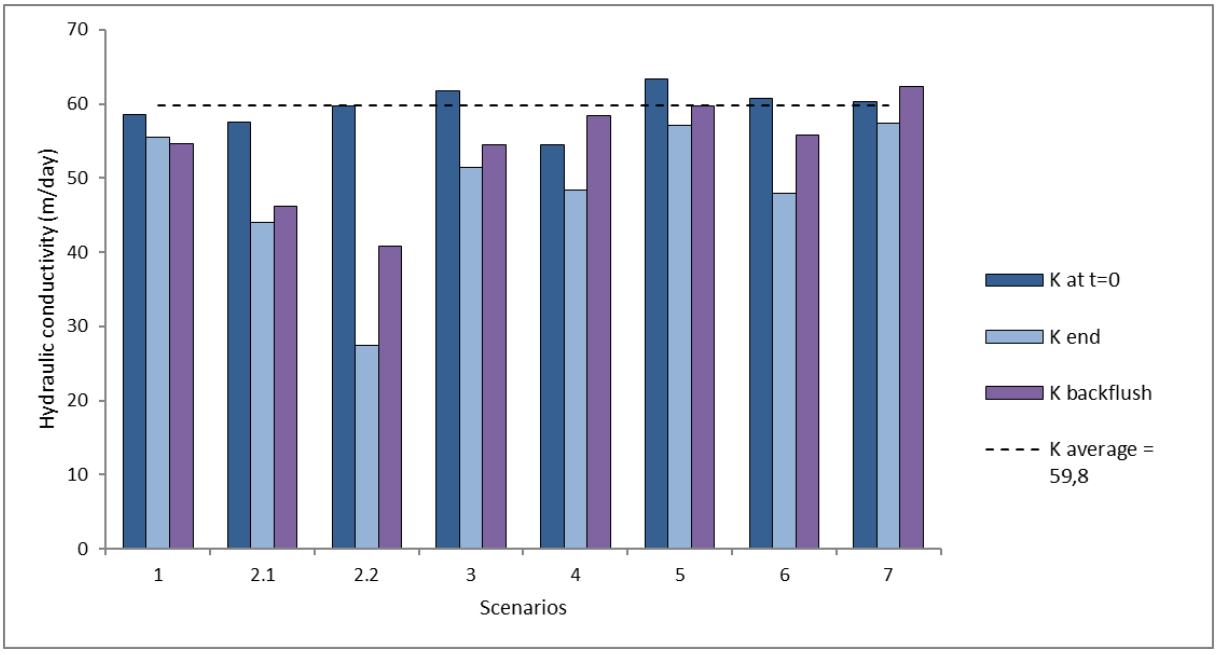

Figure 14 K at 3 different moments during the experiment. The starting K at t = 0, K after infiltration of ACC and flushing with water and K when flow direction is reversed to simulate the pumping after infiltration of ACC. K average is the average of the initial K's

4.2.4 Reactive zone creation and evolution

The goal of near well filtration is creating a reactive zone of ACC around that well. Figure 15 shows the created ACC enriched zones for the different scenarios.

Unfortunately, the pictures are not always very clear. Differences in lighting and angle at the moment the pictures were taken, have resulted in differences in colors and contrasts between pictures. However, this visualization is still valuable and certain differences between scenario's are clear enough.

In In the case of scenario 1 and 7, the boundary of the reactive zone is a more defined boundary than in the other scenario's. The rest of the column in scenario 1 and 7 has still the color of the mother material while in the other scenario's the rest of the column seems to be darker colored as well. This is also in accordance with the BTC's (figure 12) and mass balance (figure 11) which showed no passage of ACC's through the column.

In the case of the stabilized suspensions (scenario 2.1-6) not only the identified strongly ACC enriched zone contains ACC's, but also the conceding zone of the column is darker colored. This means that with the help of a stabilizer, the reactive zone can extend further into the aquifer. The immobilized ACC's in this conceding zone are the smallest particles stable in suspension like the ACC's in the effluent. Busch et al. (2014) conducted column experiments with CMC stabilized carbo-nZVI and also found the immobilization of the particles to be non lineair. They identified a strongly enriched zone at the beginning as well, followed by a lesser enriched zone. Also in deposition profiles of carboxyl colloids from column experiments conducted by Bradford et al. (2002, 2006, 2007), immobilization was highest in the first part and after that equal colloid distribution in the rest of the column.

Figure 15 Visualization of the created ACC enriched zones during the experiments. The first column shows a clean sand body for comparison. The blue dotted lines indicate marked points on the column. The columns were filled up till 84 cm. The green lines are indicating up till where the sand is clearly darker than the mother material.

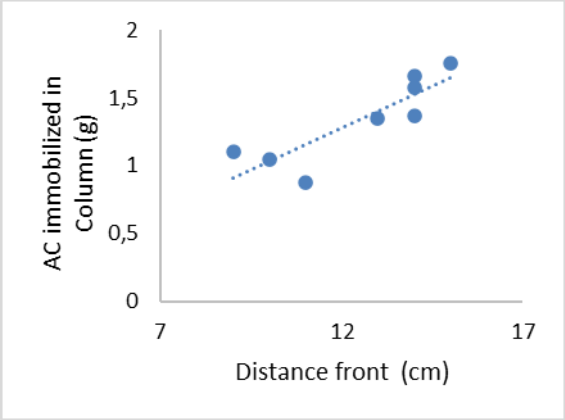

Figure 16 The amount of immobilized AC versus the distance of the front.

The size of the strongly enriched zone is also related to the amount of ACC that is immobilized in the column (figure 16) . In the cases where more ACC was infiltrated into the column, the front of the reactive zone progressed further.

Figure 17 illustrates the position of the strongly enriched zone during the experiments. These positions were base on pictures made during the experiment and are somewhat subjective. It does not show a clear relation over time either. The untreated ACC suspension (scenario 1) for example seems to show a slowing down of the progression of the zone over time. Other scenario's like when flow velocity is reduced (scenario 6) for example shows a more linear course.

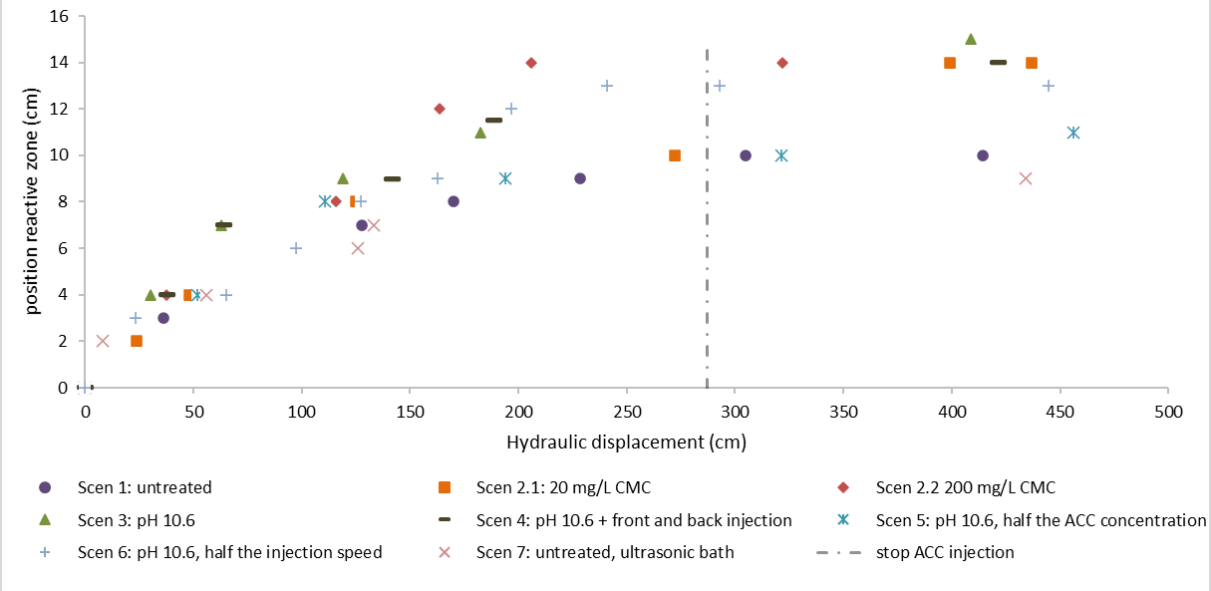

Figure 17 The position of the strongly enriched zone versus the total hydraulic displacement for all scenario's. Note that the position is based on pictures made during the experiment and thus subjective.

4.3 Translation of column experiment to the field

Transferring the results of the column experiments to an aquifer system in the field is difficult. The circumstances in and characteristics of an aquifer vary per location and thus the boundary conditions set up in the column experiments differ from the conditions in the field. The column experiments showed that injection velocity plays an important role in the formation of the reactive zone and the hydraulic conductivity. Figure 18 shows maximum allowed flow velocity around the borehole wall for an aquifer with the same K as the Corle sand in our experiments. The majority of the column experiments was carried out with a linear Darcy flow velocity of 4.2 m/hour, which is above the most applied maximum flow velocity according to Sichardt but below the rule of Huisman and the NVO subtraction norm. The scenario where a lower linear flow velocity was used, is just under the rule of Sichardt. While in the column experiments flow velocity was constant over the full length of the

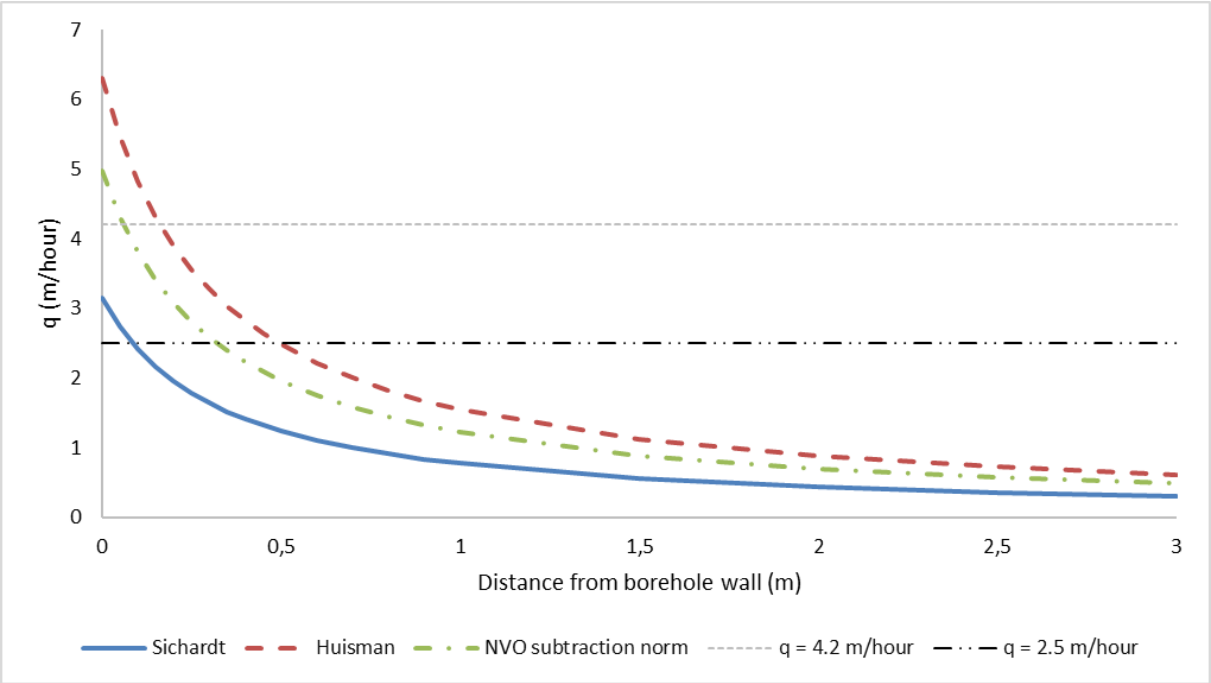

Figure 4 The maximum allowed flow velocities around a pumping well with standard measurements according to 3 different formula's in comparison to the flow velocities in the column experiments. The measurements of the pumping well used here are: D = 0,65 m and L = 10.

column, flow around a pumping well is radial and flow velocities decrease very rapid with distance from the well (figure 18). This might have an effect on the immobilization of particles in the aquifer and can enhance straining. However, the column experiments showed that the majority of deposition is in the first few centimeters of the sand, where flow velocities are still rather high in a radial flow field. The decrease in flow velocity might even stimulate the deposition of the smaller particles that were able to pass through the column in the column experiments.

The radial flow in the subsurface probably also results in mixing an dilution at the injection front. If stabilization with a high pH deionized water is applied, mixing with the groundwater will have a destabilizing effect because it lowers the pH and increases the ionic strength. The chemistry of the aquifer won't be altered too much, as groundwater buffers the high pH of the deionized water very easily. This means there are also no residuals with this treatment opposed to stabilization with CMC. It might be not desirable to have a polymer as CMC in large quantities around the pumping well. When CMC is biodegraded in the subsurface, this can result in a presence of undesirable microbes (Nie et al., 2014).

Another factor that was not looked at in the column experiments but is very important in the immobilization of particles in a porous medium is the size of the colloids compared to pore size (Bradford et al., 2002; Bradford et al., 2005; Bradford et al., 2007; Busch et al., 2014). If an aquifer has a very fine porous structure, the ACC's should also be smaller to prevent complete straining and thus clogging of the pores. On the other side, if an aquifer has a very course porous structure, the ACC's should not be to small to optimize retention.

Conclusion

Experimental batch suspension tests and column experiments were conducted and gave some valuable insights about the controls in ACC suspension stability and the immobilization of ACC's in a sandy porous medium.

Three different ACC types (NORIT SA UF, NORIT SAE SUPER and NORIT ASPEC E 153) were assessed for their stability in suspension. NORIT SA UF showed to be most stable in suspension especially in high pH (10,6-11) deionized water. An increase in ionic strength had a negative effect on the suspension stability. CMC also increased the ACC stability in suspension significantly. Furthermore, mixing intensity plays an important role in the initial separation of particles in suspension and consequently suspension stability both immediately after mixing as well as over a longer time period afterwards.

The suspensions in tap water without a stabilizer, mixed with a blender (scenario 1) and dispersed in an ultrasonic bath (scenario 7) gave very similar results. In both scenarios around the same amount of ACC was immobilized in the column and the decrease in hydraulic conductivity was limited. The absence of a stabilizer prevented the particles to travel far into the column and the zone where ACC retention occurred, was only a few centimeters long.

Stabilization with CMC (scenario 2.1 & 2.2) resulted in less settling of ACC in the batch suspension, resulting in a higher amount of ACC in the column. ACC's also infiltrated further into the column and ACC retention occurred over the full length of the column. However the hydraulic conductivity of the column had a far larger decrease, especially when the concentration of CMC was higher (scenario 2.2).

Stabilization with high pH in deionized water (scenario 3-6) resulted in a high amount of ACC infiltrated and enabled the particles to travel further through the column and let to immobilization of ACC's over the full length of the column. A decrease in flow velocity resulted in a larger decrease in hydraulic conductivity, probably due to increased straining because of lower fluid drag forces at lower flow velocities. Also less ACC was infiltrated into the column because ACC in the batch suspension in the container had more time to settle. A lower ACC concentration only led to less ACC being infiltrated into the column. There was also no significant effect from a front and back injection of alkaline deionized water.

For the stabilized suspensions (scenario 2.1-6) particle immobilization was high in the first section of the column, followed by a seemingly equal distribution of ACC's over the rest of the column. Remobilization during reversed flow was limited in al the scenario's which is very important in creating a stable reactive zone

Stabilization of ACC suspension with high pH deionized water for infiltration in the subsurface is very promising based on the results from the column experiments. Transferring the results of the column experiments to an aquifer system in the field is difficult as lab conditions are always idealized compared to the field. However, these results can help in future research regarding the mechanics in creating a reactive zone in the subsurface for subsurface groundwater treatment.

Literature

Austin, R. W., 1973. Problems in Measuring Turbidity as a Water Quality Parameter. U.S. EPA Seminar on Methodology for Monitoring the Marine Environment. October 16-18, 1973, Seattle, Washington.

Babić, B. M., Milonjić, S. K., Polovina, M. J., & Kaludierović, B. V. (1999). Point of zero charge and intrinsic equilibrium constants of activated carbon cloth. Carbon, 37(3), 477-481.

Başar, C. A., Karagunduz, A., Keskinler, B., & Cakici, A. (2003). Effect of presence of ions on surface characteristics of surfactant modified powdered activated carbon (PAC). Applied surface science, 218(1-4), 170-175.

Bjelopavlic, M., Newcombe, G., & Hayes, R. (1999). Adsorption of NOM onto activated carbon: effect of surface charge, ionic strength, and pore volume distribution. Journal of colloid and interface science, 210(2), 271-280.

Bradford, S. A., Yates, S. R., Bettahar, M., & Simunek, J. (2002). Physical factors affecting the transport and fate of colloids in saturated porous media. Water resources research, 38(12), 63-1.

Bradford, S. A., Simunek, J., Bettahar, M., van Genuchten, M. T., & Yates, S. R. (2003). Modeling colloid attachment, straining, and exclusion in saturated porous media. Environmental science & technology, 37(10), 2242-2250.

Bradford, S. A., Simunek, J., Bettahar, M., Van Genuchten, M. T., & Yates, S. R. (2006). Significance of straining in colloid deposition: Evidence and implications. Water Resources Research, 42(12).

Bradford, S. A., Torkzaban, S., & Walker, S. L. (2007). Coupling of physical and chemical mechanisms of colloid straining in saturated porous media. Water Research, 41(13), 3012-3024.

Busch, J., Meißner, T., Potthoff, A., & Oswald, S. E. (2014). Transport of carbon colloid supported nanoscale zero-valent iron in saturated porous media. Journal of contaminant hydrology, 164, 25-34.

Busch, J., Meißner, T., Potthoff, A., Bleyl, S., Georgi, A., Mackenzie, K., Trabitzsch, R., Werban, U & Oswald, S. E. (2015). A field investigation on transport of carbon-supported nanoscale zero-valent iron (nZVI) in groundwater. Journal of contaminant hydrology, 181, 59-68.

Chingombe, P., Saha, B., & Wakeman, R. J. (2005). Surface modification and characterisation of a coal-based activated carbon. Carbon, 43(15), 3132-3143.

Du, B., Li, J., Zhang, H., Chen, P., Huang, L., & Zhou, J. (2007). The stabilization mechanism of acidified milk drinks induced by carboxymethylcellulose. Le Lait, 87(4-5), 287-300.

Eisma, D. (1986). Flocculation and de-flocculation of suspended matter in estuaries. Netherlands Journal of Sea Research, 20(2-3), 183-199.

Faisal, A. A. H., Sulaymon, A. H., & Khaliefa, Q. M. (2018). A review of permeable reactive barrier as passive sustainable technology for groundwater remediation. International Journal of Environmental Science and Technology, 15(5), 1123-1138.

Fan, D., Gilbert, E. J., & Fox, T. (2017). Current state of in situ subsurface remediation by activated carbon-based amendments. Journal of environmental management, 204, 793-803.

Fu, F., Dionysiou, D. D., & Liu, H. (2014). The use of zero-valent iron for groundwater remediation and wastewater treatment: a review. Journal of hazardous materials, 267, 194-205.

Gehrke, I., Geiser, A., & Somborn-Schulz, A. (2015). Innovations in nanotechnology for water treatment. Nanotechnology, science and applications, 8, 1.

Georgi, A., Schierz, A., Mackenzie, K., & Kopinke, F. D. (2015). Colloidal activated carbon for in-situ groundwater remediation—Transport characteristics and adsorption of organic compounds in water-saturated sediment columns. Journal of contaminant hydrology, 179, 76-88.

Gupta, V. K., Ali, I., Saleh, T. A., Nayak, A., & Agarwal, S. (2012). Chemical treatment technologies for waste-water recycling—an overview. Rsc Advances, 2(16), 6380-6388.

Hahn, M. W., & O'Melia, C. R. (2004). Deposition and reentrainment of Brownian particles in porous media under unfavorable chemical conditions: Some concepts and applications. Environmental Science & Technology, 36, 210–220.

Hanak, E., Mount, J., Chappelle, C., Lund, J., Medellín-Azuara, J., Moyle, P., & Seavy, N. (2015). What if California's drought continues. Public Policy Institute of California, 6894726-181.

Hartog, N. (2016). 3.2 Near-well subsurface treatment technologies for sustainable drinking water production. Filtration Materials for Groundwater: A Guide to Good Practice, 59.

He, F., Zhang, M., Qian, T., & Zhao, D. (2009). Transport of carboxymethyl cellulose stabilized iron nanoparticles in porous media: Column experiments and modeling. Journal of colloid and interface science, 334(1), 96-102.

Hogg, R. (2000). Flocculation and dewatering. International Journal of Mineral Processing, 58(1-4), 223-236.

Houtman, C. J., Kroesbergen, J., Lekkerkerker-Teunissen, K., & van der Hoek, J. P. (2014). Human health risk assessment of the mixture of pharmaceuticals in Dutch drinking water and its sources based on frequent monitoring data. Science of the Total Environment, 496, 54-62.

Hunter, R. J. (1993). Introduction to modern colloid science (Vol. 7). Oxford: Oxford University Press.

Kim, H. J., Lee, S. H., Lee, J. H., & Jang, S. P. (2015). Effect of particle shape on suspension stability and thermal conductivities of water-based bohemite alumina nanofluids. Energy, 90, 1290-1297.

Kirk, J. T. 0., 1994. Light and Photosynthesis in Aquatic Ecosystems. (Second Edition). Cambridge University Press, New York, New York. 509 pp.

Kocur, C. M., Chowdhury, A. I., Sakulchaicharoen, N., Boparai, H. K., Weber, K. P., Sharma, P., ... & O'Carroll, D. M. (2014). Characterization of nZVI mobility in a field scale test. Environmental science & technology, 48(5), 2862-2869.

Krasner, S. W., & Amy, G. (1995). Jar-test evaluations of enhanced coagulation. Journal-American Water Works Association, 87(10), 93-107.

Kümmerer, K., Dionysiou, D. D., Olsson, O., & Fatta-Kassinos, D. (2019). Reducing aquatic micropollutants–Increasing the focus on input prevention and integrated emission management. Science of The Total Environment, 652, 836-850.

Li, P., He, X., & Guo, W. (2019). Spatial groundwater quality and potential health risks due to nitrate ingestion through drinking water: A case study in Yan'an City on the Loess Plateau of northwest China. Human and Ecological Risk Assessment: An International Journal, 1-21.

Microdyn Nadir: advanced separation technologies (2017). Troubleshooting Jar Testing Procedure. Form No: TSG-T-008 // Revision: B // Date: May 25, 2017

Napper, D. H. (1977). Steric stabilization. Journal of colloid and interface science, 58(2), 390-407.

Newcombe, G., Hayes, R., & Drikas, M. (1993). Granular activated carbon: importance of surface properties in the adsorption of naturally occurring organics. Colloids and Surfaces A: Physicochemical and Engineering Aspects, 78, 65-71.

Niels Hartog, Roberta Hofman-Caris, Cheryl Bertelkamp, Martin Bloemendaal, Luc Palmen (2018). ondergronds zuiveren: verkenning van toepasbaarheid in de praktijk. KWR, BTO-Rapport.

NOS Nieuws (12-09-2019). Drinkwater bronnen steeds meer vervuild. From: https://nos.nl/artikel/2301365-drinkwaterbronnen-nederland-steeds-meer-vervuild.html

Nie, H., Liu, M., Zhan, F., & Guo, M. (2004). Factors on the preparation of carboxymethylcellulose hydrogel and its degradation behavior in soil. Carbohydrate Polymers, 58(2), 185-189.

Obiri-Nyarko, F., Grajales-Mesa, S. J., & Malina, G. (2014). An overview of permeable reactive barriers for in situ sustainable groundwater remediation. Chemosphere, 111, 243-259.

Olson, E. (2012). Zeta potential and colloid chemistry. Journal of GXP Compliance, 16(1), 81.

Park, J. B., Lee, S. H., Lee, J. W., & Lee, C. Y. (2002). Lab scale experiments for permeable reactive barriers against contaminated groundwater with ammonium and heavy metals using clinoptilolite (01-29B). Journal of hazardous materials, 95(1-2), 65-79.

Perrich, J.R., 1981. Activated Carbon Adsorption for Wastewater Treatment, first ed. CRC PRESS INC, Boca Raton, FL.

Ponnamperuma, F. N., Tianco, E. M., & Loy, T. A. (1966). Ionic strengths of the solutions of flooded soils and other natural aqueous solutions from specific conductance. Soil Science, 102(6), 408-413.

Regenesis, 2016. PlumeStop® Liquid Activated Carbon White Paper: Securing Rapid Contaminant Reduction and Accelerated Bioremediation Using a Dispersive Injectable Reagent. http://regenesis.com/technical/plumestop-white-paper/.

Salgin, S., Salgin, U., & Bahadir, S. (2012). Zeta potentials and isoelectric points of biomolecules: the effects of ion types and ionic strengths. Int. J. Electrochem. Sci, 7(12), 12404-12414.

Sjerps, R. M., ter Laak, T. L., & Zwolsman, G. J. (2017). Projected impact of climate change and chemical emissions on the water quality of the European rivers Rhine and Meuse: A drinking water perspective. Science of the Total Environment, 601, 1682-1694.

Sjerps, R. M., Kooij, P. J., van Loon, A., & Van Wezel, A. P. (2019). Occurrence of pesticides in Dutch drinking water sources. Chemosphere, 235, 510-518.

Smeets, P. W. M. H., Medema, G. J., & Van Dijk, J. C. (2009). The Dutch secret: how to provide safe drinking water without chlorine in the Netherlands. Drinking Water Engineering and Science, 2(1), 1-14.

Sorengard, M., Kleja, D. B., & Ahrens, L. (2019). Stabilization of per-and polyfluoroalkyl substances (PFASs) with colloidal activated carbon (PlumeStop®) as a function of soil clay and organic matter content. Journal of environmental management, 249, 109345.

Stumm, W. (1992). Chemistry of the solid-water interface: processes at the mineral-water and particle-water interface in natural systems. John Wiley & Son Inc..

Thiruvenkatachari, R., Vigneswaran, S., & Naidu, R. (2008). Permeable reactive barrier for groundwater remediation. Journal of Industrial and Engineering Chemistry, 14(2), 145-156.

Trefalt, G., & Borkovec, M. (2014). Overview of DLVO theory. Laboratory of Colloid and Surface Chemistry, University of Geneva, Switzerland, 1-10.

Trefalt, G., Palberg, T., & Borkovec, M. (2017). Forces between colloidal particles in aqueous solutions containing monovalent and multivalent ions. Current Opinion in Colloid & Interface Science, 27, 9-17.

Speksnijder C. (11-09-2019). Raakt ons drinkwater op? Waterbedrijven slaan alarm over de Maas. From: https://www.volkskrant.nl/nieuws-achtergrond/raakt-ons-drinkwater-op-waterbedrijven-slaan-alarm-over-de-maas~bba9f24e4/

Vitens (JAN-MRT 2020). Waterkwaliteits overzicht Tull en `t Waal. https://www.vitens.nl/service/waterkwaliteit/waterkwaliteitsoverzichten

Wallace, S. H., Shaw, S., Morris, K., Small, J. S., Fuller, A. J., & Burke, I. T. (2012). Effect of groundwater pH and ionic strength on strontium sorption in aquifer sediments: Implications for 90Sr mobility at contaminated nuclear sites. Applied Geochemistry, 27(8), 1482-1491.

Zhan, J., Sunkara, B., Le, L., John, V. T., He, J., McPherson, G. L., Piriniger, G. & Lu, Y. (2009). Multifunctional colloidal particles for in situ remediation of chlorinated hydrocarbons. Environmental science & technology, 43(22), 8616-8621.

Zeta-Meter, Inc., Zeta Potential: A Complete Course in 5 Minutes, http://www.zeta-meter.com/5min.pdf